

## Survey report

***MS Eros, MS Kings Bay MS Vendla 13.-25.02.2019***



## **Distribution and abundance of Norwegian spring-spawning herring during the spawning season in 2019**

**By Aril Slotte, Are Salthaug, Erling Kåre Stenevik, Sindre Vatnehol and Egil Ona**

Institute of Marine Research (IMR), P. O. Box 1870 Nordnes, N-5817 Bergen, Norway

## Contents

Summary .....	3
Survey participants 13-25.02.2019: .....	4
Introduction .....	4
Material and methods .....	5
Survey design .....	5
Biological sampling.....	6
Environmental sampling .....	6
Echo sounder data .....	6
Abundance estimation methods .....	7
Results and discussion.....	11
Spatial distribution and acoustic densities .....	11
Depth distribution.....	11
Estimated biomass index .....	11
Estimated abundance index by age .....	11
Trends in biomass index and abundance index by age 2015-2018 .....	12
Geographical variation in biomass and abundance index by age.....	12
Maturation status .....	13
Geographical variation in temperatures experienced by the herring.....	14
Quality of the survey for abundance estimation.....	14
Acknowledgements .....	16
References .....	16
Tables .....	19
Figures.....	21
Annex 1. Calibration results and settings.....	35
Annex 2. Sonar report .....	37
Annex 3. Corrections for air bubble attenuation on keel-mounted echo sounders .....	39
Annex 4. TS measurements.....	47
Annex 5. Examples of acoustic registrations with EK80 at Kings Bay.....	49

## Summary

During the period 13-25<sup>th</sup> of February 2019 the spawning grounds of NSS herring from Møre (62°N) to the borderline Troms-Finnmark at Tromsøflaket (71°) were covered acoustically by the commercial vessels MS *Eros*, MS *Kings Bay* and MS *Vendla*. The survey was carried out under variable weather conditions; very rough conditions in the beginning, improving over the survey, yet with very few days with good conditions. This led to some problems with acoustic registrations, to a degree that some corrections of data due to air-bubble attenuation was necessary. The trawling for verification of acoustic registrations and for sampling of herring was also to some degree hindered by the rough weather during the survey. Still, the data recorded during the survey were considered to be of adequate quality. As in 2018, most of the herring in 2019 were distributed in deep layers from 150-300 m depth. In addition, sonar investigations indicated that that echo sounder biomass estimations were not seriously biased by unaccounted fraction of herring in the upper layers (i.e. vessel avoidance and/or distribution of fish in the blind zone between the surface and the echo sounder transducer). The estimated biomass index of 4.25 was a 30% increase from 2018, but with a bit higher (yet still low) uncertainty of CV=10.0% compared with the very low CV=7.4 % in 2018. The increase in the biomass index from last year seems to be a general result of more fish being captured by the survey across ages in 2019 than in 2018 (indication of a year effect), but the largest increase in biomass was for the 2013 year class, a 60 % increase which also was attributed to body growth. The 2013 year class was clearly the most abundant year class in the survey contributing with 26 % in numbers, but fish from older year classes 2006 and 2004 were still present in relatively high numbers contributing with 13 % each. The first significant herring observations was recorded north on the Møre shelf at Buagrunnen 63°N, and from here and northwards the herring was distributed along the coast and observed on most of the transects as far as south of Tromsøflaket 70°30N. About 69 % of the biomass was found between 63° and 67°30N, and the rest was found up to 71°N. The presence of the 2013 year class clearly increased northwards, predominating north of 67°N. The subjective scaling of maturation and GSI (% gonad weight relative to total weight) was quite similar over the survey area, indicating that the herring were still maturing and that timing of main spawning event was after the survey.

**Survey participants 13-25.02.2019:**MS *Eros*

Aril Slotte	Survey leader
Jan Frode Wilhelmsen	Instrument/Acoustics
Sindre Vatnehol	Scientist/Acoustics
Ståle Kolbeinson	Biology
Jostein Røttingen	Biology

MS *Kings Bay*

Erling Kåre Stenevik	Survey coordinator
Egil Ona	Head of acoustics
Jarle Kristiansen	Instrument/Acoustics
Guosong Zhang	Instrument/Acoustics
Stine Karlson	Biology
Ørjan Sørensen	Biology

MS *Vendla*

Are Salthaug	Survey leader
Reidar Johannesen	Instrument/Acoustics
Kåre Tveit	Instrument/Acoustics
Valantine Anthonypillai	Biology
Adam Custer	Biology

**Introduction**

Acoustic surveys on NSS herring during the spawning season has been carried out regularly since 1988, with some breaks (in 1992-1993, 1997, 2001-2004 and 2009-2014). In 2015 the survey was initiated again partly based on the feedback from fishermen and fishermen's organizations that IMR should conduct more surveys on this commercially important stock. Since then this has continued with a survey design using three commercial vessels, and IMR has contracted the same vessels to run this survey during the period 2017-2020. The ICES WKPELA benchmark in 2016 decided to use the data from this time series as input to the stock assessment, together with the ecosystem survey in the Norwegian Sea in May in addition to catch data, meaning that the results of the survey have significant influence on quota advice.

Hence, the objective of the NSS spawning survey 2019 was to continue the index for use in the ICES WGWIDE stock assessment, more specifically to estimate indices of abundance at age and biomass during the period of spawning migration from wintering areas at/off the northern

Norwegian coast and in the Norwegian Sea towards the coastal spawning ground further south. Finally, it was also a purpose that the results of the survey should be compared with recent surveys with comparable effort and design during 2015-2019.

## **Material and methods**

### *Survey design*

During the period 13-25<sup>th</sup> of February 2019 (exact same period as in 2017-2018) the spawning grounds from Møre (62°N) to Troms (71°N) were covered acoustically by the commercial fishing vessels *MS Eros*, *MS Kings Bay* and *MS Vendla*.

The survey was planned based on the information we held from the distribution of the fishery during the autumn 2018 up to the survey start 13. February 2019 (Figure 1). The fishery prior to the survey start in 2019 was indicating that the herring wintering in the Norwegian Sea were entering the coast in the Træna deep south of Røst and following the eastern shelf edge 200 m depth southwards from Træna as also observed in 2016-2018. This information also suggested that smaller and younger herring recruiting to the spawning stock initiated their spawning migration from wintering grounds further north of 70°N west of Tromsøflaket and in Kvænangen fjord area, which was the basis for the planned survey coverage this far north. As seen from Figure 1, the fishery had already started at Buagrunnen (63°N) at the onset of survey 13 February in 2018, whereas in 2019 the fishery did not start in this area until a couple of days after the survey started. It was discussed among fishermen that the herring they were fishing at Buagrunnen came directly from the Norwegian Sea from the west, not following the southward migration along the shelf from Røst. This is difficult to disprove, but the recordings from the survey (both biomass and size of herring) suggest that herring observed from Buagrunnen and northwards clearly may have attributed to the fishery developing at Buagrunnen after the survey passed the area.

The survey design followed a standard stratified design (Jolly and Hampton 1990), where the survey area was stratified before the survey start according to the expected density and age structures of herring (Figure 2). With exception of stratum 14, all strata this year was covered with a zig zag design instead of parallel west-east transects each (Figure 3). The introduction of a zig-zag design started in 2018, and it was based on the wish to reduce the uncertainty

related to stock coverage, using more of the survey time on transects and thereby increasing the survey coverage. In 2015-2017, a significant part of the survey time was used as transport between transects, whereas in 2018-2019 insignificant time was used on transport. Each straight line in the zig-zag design were considered as transects and primary sampling units (Simmonds and MacLennan 2008), with uniform coverage of strata and a random starting position.

### *Biological sampling*

Trawl sampling was carried out on a regular basis during the survey to confirm the acoustic observations and to be able to give estimates of abundance for different size and age groups. The positions of the trawl hauls are shown in Figure 3. The following variables of individual herring were analysed for each station with herring catch: Total weight ( $W$ ) in grams and total length ( $L_T$ ) in cm (rounded down to the nearest 0.5 cm) of up to 100 individuals per sample. In addition, age from scales, sex, maturity stage, stomach fullness and gonad weight ( $W_G$ ) in grams were measured in up to 50 individuals per sample. The maturation stages were determined by visual inspection of gonads as recommended by ICES (Anon. 1962): immature = 1 and 2, early maturing = 3, late maturing = 4, ripe = 5, spawning = 6, spent = 7 and resting/recovering = 8. Data from the subjective evaluation of maturation stages were used to split between immature and mature herring in the estimation of spawning stock biomass (SSB), as well as to demonstrate spatial differences in maturation. The gonadosomatic index ( $GSI = \text{gonad weight} / \text{total weight} \times 100$ ) was also used to demonstrate spatial differences in maturation along the coast.

### *Environmental sampling*

CTD casts (using Seabird 911 systems) were taken by MS Eros and Vendla, spread out in the survey area (Figure 3).

### *Echo sounder data*

Multifrequency (18, 38, 70, 120, 200 kHz) acoustic data were recorded with a SIMRAD EK 60 echo sounder and echo integrator on board Eros and Vendla, and SIMRAD EK 80 on board Kings Bay. All three vessels were calibrated at the tip of the fishing pier in Ålesund prior to the survey according to standard methods (Foote et al., 1987), adjusted for split beam methods as

described in Ona (1999) and (Demer et al., 2015). The calibration reports of each vessel are shown in Annex 1. The low frequency sonars were not calibrated. The intention was only to use the sonar data for studies of potential issues with herring in blind zone close to the surface or avoidance, not for biomass estimations of schools. Hence, a new calibration of the sonars was not considered necessary. For details on the use of sonar and data storage, see sonar report in Annex 2.

LSSS, Large Scale Survey System (Korneliussen et al., 2006) was applied for the interpretation of the multi-frequency data. The recorded area echo abundance, i.e. the nautical area backscattering coefficient (NASC) (MacLennan et al., 2002), was interpreted and distributed to herring and ‘other’ species at 38 kHz. Various characteristics of the acoustic recordings like frequency response (Korneliussen & Ona, 2002) and visual appearance were used to identify herring from other targets.

In 2019 the survey suffered from relatively bad weather conditions compared with 2018. During conditions where the vessels had to survey against strong winds, acoustic registrations on some transects were significantly influenced by air bubble attenuation. This was corrected for during the scrutinization of the data in LSSS, and the problems and methods used to adjust is described in Annex 3, see also Annex 5 for more examples of echograms with bubble attenuation problems.

#### *Abundance estimation methods*

The acoustic density values were stored by species category in nautical area scattering coefficient (NASC) [ $\text{m}^2 \text{ n.mi.}^{-2}$ ] units (MacLennan et al. 2002) in a database with a horizontal resolution of 0.1 nmi and a vertical resolution of 10 m, referenced to the sea surface. To estimate the mean and variance of NASC, we use the methods established by Jolly and Hampton (1990) and implemented in the software StoX. The primary sampling unit is the sum of all elementary NASC samples of herring along the transect multiplied with the resolution distance. The transect ( $t$ ) has NASC value ( $s$ ) and distance length  $L$ . The average NASC ( $S$ ) in a stratum ( $i$ ) is then:

$$\hat{S}_i = \frac{1}{n_i} \cdot \sum_{t=1}^{n_i} w_{it} s_{it} \quad (1)$$

where  $w_{it} = L_{it} / \bar{L}_t$  ( $t= 1,2,.. n_i$ ) are the lengths of the  $n_i$  sample transects, and

$$\bar{L}_t = \frac{1}{n_i} \sum_{t=1}^{n_i} L_{it} \quad (2)$$

The final mean NASC is given by weighting by stratum area, A;

$$\hat{S} = \frac{\sum_i A_i \hat{S}_i}{\sum_i A_i} \quad (3)$$

Variance by stratum is estimated as:

$$\hat{V}(\hat{S}_i) = \frac{n}{n_i - 1} \sum_{t=1}^n w_{it}^2 (s_t - \bar{s})^2 \quad \text{with } \bar{s}_i = \frac{1}{n_i} \cdot \sum_{t=1}^{n_i} s_t \quad (4)$$

Where  $w_{it} = L_{it} / \bar{L}_t$  ( $t= 1,2,.. n_i$ ) are the lengths of the  $n_i$  sample transects.

The global variance is estimated as

$$\hat{V}(\hat{S}) = \frac{\sum_i A_i^2 \hat{V}(\hat{S}_i)}{\left( \sum_i A_i \right)^2} \quad (5)$$

The global relative standard error of NASC

$$RSE = 100 \sqrt{\frac{\hat{V}(\hat{S})}{N}} / \hat{S} \quad (6)$$

where N is number of strata.

In order to verify acoustic observations and to analyse year class structure over the surveyed area, trawling was carried out regularly along the transects (Figure 3). All trawl stations with herring were used to derive a common length distribution for all transect within the respective strata. All stations had equal weight.

Relative standard error by number of individuals by age group was estimated by combining Monto Carlo selection from estimated NASC distributions by stratum with bootstrapping techniques of the assigned trawl stations.

The acoustic estimates presented in this report use the 38 kHz NASC, and the mean was calculated for data scrutinized as herring and collected along the transects (acoustic recordings taken during trawling, and for experimental activity are excluded). The number of herring ( $N$ ) in each length group ( $l$ ) within each stratum ( $i$ ) is then computed as:

$$N_l = \frac{f_l \cdot \hat{S}_i \cdot A_i}{\langle \sigma \rangle}$$

Where

$$f_l = \frac{n_l L_i^2}{\sum_{l=1}^m n_l L_l}$$

is the "acoustic contribution" from the length group  $L_l$  to the total energy and  $\langle s_i \rangle$  is the mean nautical area scattering coefficient [ $\text{m}^2/\text{nmi}^2$ ] (NASC) of the stratum.  $A$  is the area of the stratum [ $\text{nmi}^2$ ] and  $\sigma$  is the mean backscattering cross section at length  $L_l$ . The conversion from number of fish by length group ( $l$ ) to number by age is done by estimating an age ratio from the individuals of length group ( $l$ ) with age measurements. Similar, the mean weight by length and age grouped is estimated.

The mean target strength (TS) is used for the conversion where  $\sigma = 4\pi 10^{(\text{TS}/10)}$  is used for estimating the mean backscattering cross section. Traditionally,  $\text{TS} = 20\log L - 71.9$  (Foote 1987) has been used for mean target strength of herring during the spawning surveys, however, several papers question this mean target strength. Ona (2003) describes how the target strength of herring may change with changes with depth, due to swimbladder compression. He measured the mean target strength of herring to be  $\text{TS} = 20\log L - 2.3 \log(1 + z/10) - 65.4$  where  $z$  is depth in meters. Given that previous surveys were estimated using Foote (1987), the estimation this year was also done with this TS, for direct comparison and possible inclusion in ICES WGWIDE 2019 as another year in the time series. However, as in the 2016-2018, special measurements were made from MS Kings Bay for investigating if the mean target strength of herring during spawning is different from non-spawning herring. See Annex 4 for information

regarding these experiments which at a later stage will be used to develop a new depth dependent TS, which could be used to re-estimate all years of this survey. This will be a more realistic mean target strength for spawning herring, measured in situ, expected to remove potential bias from variable depth distribution between surveys and survey areas (see Figure 6).

The StoX software developed by IMR were used in the abundance estimation in 2019, just as in 2015-2018. StoX is an open source software developed at IMR, Norway to calculate survey estimates from acoustic and swept area surveys. The program is a stand-alone application build with Java for easy sharing and further development in cooperation with other institutes. The underlying high resolution data matrix structure ensures future implementations of e.g. depth dependent target strength and high resolution length and species information collected with camera systems. Despite this complexity, the execution of an index calculation can easily be governed from user interface and an interactive GIS module, or by accessing the Java function library and parameter set using external software like R. Accessing StoX from external software may be an efficient way to process time series or to perform boot-strapping on one dataset, where for each run, the content of the parameter dataset is altered. Various statistical survey design models can be implemented in the R-library, however, in the current version of StoX the stratified transect design model developed by Jolly and Hampton (1990)<sup>i</sup> is implemented.

### *Sonar data and analyses*

Data from Simrad low-frequency sonars were logged onboard all vessels with the objective to measure the presence and magnitude of potential bias related to vertical distribution (fish in blind zone above the echo sounder transducer) and avoidance behaviour of the herring relative to the presence of the vessel. Data from fisheries sonars have been collected from all participating vessels since 2015. Methods to quantify or evaluate the extend of these biases are presently being developed. See Annex 2 for more information on sonar logging and data.

## Results and discussion

### *Spatial distribution and acoustic densities*

The distribution and densities of herring in the area covered in 2019 was quite similar to that observed in 2018, relatively evenly distributed along the coast 63-71°N, yet with some high density areas around Halten/Sklinna banks (64°30'-66°N) and south western part of Vesterålen banks (67°30'N-68°30'N) (Figures 4 and 5).

### *Depth distribution*

As in 2018 most of the herring in 2019 were distributed in deep acoustic layers at 150-300 m depth south of 67°N, whereas further north along the western part of the Vesterålen shelf area and northwards along the coast high densities were also observed closer to the surface during periods of darkness (Figure 6). Several examples of acoustic registrations of herring in the survey area using EK80 echo sounder are given in Annex 5.

### *Estimated biomass index*

The estimate of a total stock biomass index using StoX, to be treated as a relative one, was 4.25 in 2019 (Table 1) with a reasonably low uncertainty (CV = 10.0%). A 33 % bulk of the herring biomass was found in the area Halten and Sklinna (64°30'-66°N), but also 32% was found along Vesterålen and further north (north of 67°30'N) (Figure 7, Table 2), suggesting that these areas were also important for spawning. The biomass index in 2019 was a 30% increase from 2018 when it was estimated to be 3.3 with a very low uncertainty (CV = 7.5%). The trends in the total abundance and biomass index since 2015 shows a decline until 2017, after which a flattening in 2018 and an increase in 2019 (Figure 8).

### *Estimated abundance index by age*

The 2013 year class was clearly the most abundant year class in the survey in 2019 contributing with 26 % in numbers, but fish from older year classes (2006 and 2004) were still present in relatively high numbers contributing with 13% each (Figure 9, Table 3). The estimated

abundance index by age appeared with low uncertainty and CVs mostly ranging between 15-20 % for ages 4-15, whereas the estimates were less precise with CVs above 25% for younger and older fish (Figure 9, Table 3). This CV pattern is quite normal since few very old and very young fish are caught.

#### *Trends in biomass index and abundance index by age 2015-2018*

A more detailed inspection of the trends in number of fish per year class over all surveys 2015-2018 clearly demonstrate a steady decrease in exploited year classes with time, but from 2018 to 2019 we see a minor increase for most year classes (Figure 10). The estimated trends in year class abundance over time is considered a sign of quality or consistency; i.e. if you see a steady decrease as a result of exploitation and natural mortality after a year class is fully recruited to the spawning stock. This is indicating that the survey captures quite well the relative trends in abundance. Still, so-called year effects (unexpected drops or increases over all year classes) in such survey indices are quite normal. The increase in biomass index from 2018 to 2019 seems to be a general result of more fish being captured by the survey across ages than in 2018. However, the largest increase in biomass was for the 2013 year class; a 60 % increase that also may be attributed to the fact that it was fully recruited to the spawning stock in 2019 and to body growth since 2018. The trends in the year classes over 2015-2019 (Figure 10) also signifies that there does not seem to be any new significant recruitment after the 2013 year class, and that 2013 is a moderate size year class compared to the 2004 year class having dominated in the spawning stock for many years.

When year classes are fully recruited to the spawning stock, the abundance indices from the survey in the Norwegian Sea in May and the following spawning survey in February should show comparable numbers. A comparison between the May survey 2018 and February survey 2019 demonstrates that the two surveys are showing the same signal in terms of present year class strengths (Figure 11).

#### *Geographical variation in biomass and abundance index by age*

The age and size of the herring was relatively stable all over the area 63-67°N, but further north size and age of the herring decreased (Figures 12-14). North of 67°N the 2013 year class predominated, and north of 69°N to especially west of Tromsøflaket in Stratum 18 the 2016

year class (3 year olds) started to contribute in high numbers (Figure 12, Table 2). This year class is expected to be the largest year class since 2004 based on surveys in the Barents Sea in recent years. The first real test to verify if this prediction is true is the 2019 ecosystem survey in May in the Norwegian Sea. Based on the results from the spawning survey, it seems that this year class already is migrating out of the Barents Sea and should be captured by the ecosystem survey in May.

The observed size dependent distribution pattern in 2019 is similar to what was observed in 2015-2018 (Slotte et al 2015, 2016, 2017, 2019). It is also in accordance with the observations in earlier years, which has been thoroughly discussed in Slotte and Dommasnes, 1997, 1998, 1999, 2000; Slotte, 1998*b*; Slotte, 1999*a*, Slotte 2001, Slotte et al. 2000, Slotte & Tangen 2005, 2006). The main hypothesis is that this could be due to the high energetic costs of migration, which is relatively higher in small compared to larger fish (Slotte, 1999*b*). Large fish and fish in better condition will have a higher migration potential and more energy to invest in gonad production and thus the optimal spawning grounds will be found farther south (Slotte and Fiksen, 2000), due to the higher temperatures of the hatched larvae drifting northwards and potentially better timing to the spring bloom (Vikebø et al., 2012).

#### *Maturation status*

No real clear geographical trends in the maturation of the herring were observed during the survey coverage and biological sampling based on subjective scaling of gonads, and by looking at the gonadosomatic index ( $GSI = \text{gonad weight} \times 100 / \text{total weight}$ ) (Figure 15). The herring seemed to be less ripe than observed in 2018, when more herring was spawning or close to spawning (Slotte et al. 2018), suggesting a later main spawning event in 2019. In 2018 there was also quite evident that herring in the northern part of the distribution tended to be less ripe (Slotte et al. 2018). This is in accordance with a general perception that the first time spawners tend to spawn later in the season, in a second wave (Slotte 2001, Slotte et al. 2000). However, in 2019 very few fish were recruit spawners, the dominating year class 2013 was fully recruited, so there were no clear indications of a second spawning wave in the north. An interesting observation was that in the area 65-67°N, herring with resting gonads (stage 8) considered to be summer spawners were present also at the coast. This was also apparent in 2018 (Slotte et al. 2018), and a possible reason is that these fish followed the main mass of spring-spawners to the coast from the wintering area in the Norwegian Sea. Alternatively, that they already were

present in the area, when the spring spawners arrived. These areas along Helgeland, Lofoten and Vesterålen is believed to be the main spawning area of the summer spawners.

#### *Geographical variation in temperatures experienced by the herring*

Temperatures experienced by herring from close to the surface and down to deeper waters than 200 m varied from 5°-8°C, clearly colder close to the surface (Figure 16). At typical spawning depths of herring 100-200 m temperature did not vary much along the coast, being rather stable at 7°-8°C as also observed in 2017-2018 (Slotte et al. 2017, 2018).

#### *Quality of the survey for abundance estimation*

In 2019 all vessels were equipped with multifrequency equipment on a drop keel. Weather conditions this year were not good, and strong wind led to periods with problems doing acoustic surveying, especially in the beginning of the survey. Hence, the acoustic data recorded was of lower quality from all three vessels than in 2018, when the surveying conditions were close to perfect (Slotte et al. 2018). The weather conditions in 2019 did not allow for a survey speed of 10 knots for the whole survey period, especially for transects running up against the wind, the vessel speed was reduced to 3-5 knots for some periods.

Even at reduced survey speed there was significant bubble attenuation. Still, given the survey coverage needed to ensure a full estimate with low uncertainty of the herring in the area, and the time available, it was decided to continue the survey during the bad weather conditions. This decision is especially linked to the potential bias in the estimates a break in the survey may lead to when covering in the direction against the migration direction of the herring. This bias was considered a larger problem than reduced quality of the acoustic data themselves, which it was possible to correct for. In Annex 3 the acoustic problems and the adjusting of bubble attenuation is described in more details.

During the survey, there was special focus on potential blind zone problems and fish avoidance, and the sonar was monitored at the same time as the echo sounder (Annex 2). The main conclusion is that we did not have a significant bias in the survey related to these factors. The main part of the estimated biomass (about 70 %) (Figure 7, Table 2) was found south of Vesterålen distributed very deep in layers both during day and night, mostly at 150-300 m depth

close to the bottom, not expecting to avoid the vessels (Figure 6). However, further north along Vesterålen and Troms at night time some strong registrations of young herring were observed close to the surface at 20-40 m depth (Figure 6). The echo sounder data suggested that they were not in the blind zone closer to the surface, as they were located 10-30 m below the transducer, and this was also supported by observations from the sonars. Still, in these northernmost strata we may have had some avoidance of these herring registrations close to the surface during night, and hence some underestimation. During daytime, however, the fish in this area were also registered very deep, typically at 200 m and deeper along the shelf edge (Figure 6), where avoidance was not expected to be a problem.

In 2019 all vessels were able to trawl, but the weather conditions also to some degree prevented trawling at acoustic registrations for verification of species or for sampling of herring in the survey area. This resulted in less sampling on acoustic registrations than in 2018, which may have resulted in a lower quality of the scrutiny process into herring and other targets, as well as lower quality on estimation of abundance index by age. Still, the scrutinizing and biological sampling was considered to be of an acceptable quality.

With regard to coverage, and potential herring outside the covered area, there were no data suggesting that this may have been a potential bias in the survey. In 2018 very few schools were registered westwards in the off-shelf wintering area (Slotte et al. 2018), where the fishery on Norwegian spring spawning herring took place prior to the survey in January. This year (2018) the herring in this area contributed with only 0.2% of the total biomass index, and it was predominated by 91% summer spawners. It was concluded that the spring spawning herring by the time of the survey coverage in 2018 already had left the wintering areas and entered the survey area. Based on the experience from 2018 as well as the experience from the earlier years 2016-2017 (Slotte et al. 2016, 2017) surveying this area, it was decided to skip this area in 2019. Instead focus was put on an area that previously has not been covered, the Trænabank area (Stratum 16), where 5% of the biomass was found (Figure 7, Table 2). This is an area that herring potentially may migrate through during the southward migration, rather than taking the main route closer to the coast along, so this is an area that should be surveyed also next years.

In summary, the acoustic and biological data recorded in 2019 were of satisfactory quality, and the distribution of the herring was wide spread leading to a good spatial coverage with many

transects in a zig-zag design and a low CV of 10.0%. Hence, the index can be recommended used for stock assessment purposes.

## Acknowledgements

Valantine Anthonypillai is thanked for the contribution with various maps to the report. Instrument and acoustic personnel Jarle Kristiansen, Jan Frode Wilhelmsen, Reidar Johannessen, Kåre Tveit and Guosong Zhang are thanked for valuable help with CTDs and acoustic data collection during the survey. Valantine Anthonypillai, Adam Custer, Jostein Røttingen, Ståle Kolbeinson, Stine Karlson and Ørjan Sørensen are thanked for their help with biological analyses and consistent age reading. All the participants and the rest of the crew on board MS *Eros*, *Kings Bay* and *Vendla* are thanked for their valuable work during the cruise. It must be emphasised that everybody from the vessels did what they possibly could to support the scientific crew; the service was splendid from the beginning to the end. Thanks to all for a very nice survey both scientifically and socially.

## References

- Aglen, A. (1983). Random errors of acoustic fish abundance estimates in relation to the survey grid density applied. *FAO Fish. Rep.* 300, 293–8.
- Foot, K. 1987. Fish target strengths for use in echo integrator surveys. *J. Acoust. Soc. Am.* 82: 981-987.
- Demer, D.A., Berger, L., Bernasconi, M., Bethke, E., Boswell, K., Chu, D., Domokos, R., *et al.* 2015. Calibration of acoustic instruments. ICES Cooperative Research Report No. 326. 133 pp.
- Jolly, G. M., and I. Hampton. "A stratified random transect design for acoustic surveys of fish stocks." *Canadian Journal of Fisheries and Aquatic Sciences* 47.7 (1990): 1282-1291.
- Korneliussen, R. J., Diner, N., Ona, E., Berger, L., and Fernandes, P. G. 2008. Proposals for the collection of multifrequency acoustic data. *ICES Journal of Marine Science*, 65: 982–994.
- Korneliussen, R. J., and Ona, E. 2002. An operational system for processing and visualizing multi-frequency acoustic data. *ICES Journal of Marine Science*, 59: 293–313.
- Korneliussen, R. J., Ona, E., Eliassen, I., Heggelund, Y., Patel, R., Godø, O.R., Giertsen, C., Patel, D., Nornes, E., Bekkvik, T., Knudsen, H.P., Lien, G. The Large Scale Survey System - LSSS. Proceedings of the 29th Scandinavian Symposium on Physical Acoustics, Ustaoset 29 January– 1 February 2006.
- Korsbrekke, K. Dingsøy, G. and Johnsen, E. In prep. Estimating variance in population characteristics with variance in transect based trawl acoustic surveys. In Prep.

- Macaulay, G.J., Vatnehol, S., Gammelsæter, O.B., Peña, H., Ona, E., 2016. Practical calibration of ship-mounted omni-directional fisheries sonars. *Methods in Oceanography* 17, 206–220.
- MacLennan, D.N., Fernandes, P., and Dalen, J. 2002. A consistent approach to definitions and symbols in fisheries acoustics. *ICES J. Mar. Sci.*, 59: 365-369.
- Ona, Egil. "An expanded target-strength relationship for herring." *ICES Journal of Marine Science: Journal du Conseil* 60.3 (2003): 493-499.
- Ona, E. (Ed). 1999. Methodology for target strength measurements (with special reference to *in situ* techniques for fish and mikro-nekton. ICES Cooperative Research Report No. 235. 59 pp.
- Slotte, A. (1998a). Patterns of aggregation in Norwegian spring spawning herring (*Clupea harengus* L.) during the spawning season. *ICES C. M.* 1998/J:32.
- Slotte, A. (1998b). Spawning migration of Norwegian spring spawning herring (*Clupea harengus* L.) in relation to population structure. Ph. D. Thesis, University of Bergen, Bergen, Norway. ISBN : 82-7744-050-2.
- Slotte, A. (1999a) Effects of fish length and condition on spawning migration in Norwegian spring spawning herring (*Clupea harengus* L.). *Sarsia* **84**, 111-127.
- Slotte, A. (1999b). Differential utilisation of energy during wintering and spawning migration in Norwegian spring spawning herring. *Journal of Fish Biology* **54**, 338-355.
- Slotte, A. 2001. Factors Influencing Location and Time of Spawning in Norwegian Spring Spawning Herring: An Evaluation of Different Hypotheses. In: F. Funk, J. Blackburn, D. Hay, A.J. Paul, R. Stephenson, R. Toresen, and D. Witherell (eds.), *Herring: Expectations for a New Millennium*. University of Alaska Sea Grant, AK-SG-01-04, Fairbanks, pp. 255-278.
- Slotte, A. & Dommasnes, A. (1997). Abundance estimation of Norwegian spring spawning at spawning grounds 20 February-18 March 1997. Internal cruise reports no. 4. Institute of Marine Research, P.O. Box. 1870. N-5024 Bergen, Norway.
- Slotte, A. & Dommasnes, A. (1998). Distribution and abundance of Norwegian spring spawning herring during the spawning season in 1998. *Fisken og Havet* **5**, 10 pp.
- Slotte, A. & Dommasnes, A. (1999). Distribution and abundance of Norwegian spring spawning herring during the spawning season in 1999. *Fisken og Havet* **12**, 27 pp.
- Slotte, A and Dommasnes, A. 2000. Distribution and abundance of Norwegian spring spawning herring during the spawning season in 2000. *Fisken og Havet* **10**, 18 pp.
- Slotte, A. & Fiksen, Ø. (2000). State-dependent spawning migration in Norwegian spring spawning herring (*Clupea harengus* L.). *Journal of Fish Biology* **56**, 138-162.
- Slotte, A. & Tangen, Ø. (2005). Distribution and abundance of Norwegian spring spawning herring in 2005. Institute of Marine Research, P. O. Box 1870 Nordnes, N-5817 Bergen ([www.imr.no](http://www.imr.no)). ISSN 1503-6294/Cruise report no. 4 2005.
- Slotte, A. & Tangen, Ø. (2006). Distribution and abundance of Norwegian spring spawning herring in 2006. Institute of Marine Research, P. O. Box 1870 Nordnes, N-5817 Bergen ([www.imr.no](http://www.imr.no)). ISSN 1503-6294/Cruise report no. 1. 2006.
- Slotte, A, Johannessen, A and Kjesbu, O. S. 2000. Effects of fish size on spawning time in Norwegian spring spawning herring (*Clupea harengus* L.). *Journal of Fish Biology* **56**: 295-310.

- Simmonds, J, and David N. MacLennan. (2005) Fisheries acoustics: theory and practice. John Wiley & Sons, 2008.
- Slotte A., Johnsen, E., Pena, H., Salthaug, A., Utne, K. R., Anthonypillai, A., Tangen, Ø and Ona, E. 2015. Distribution and abundance of Norwegian spring spawning herring during the spawning season in 2015. Survey report / Institute of Marine Research/ISSN 1503 6294/Nr. 5 – 2015
- Slotte, A., Salthaug, A., Utne, KR, Ona, E., Vatnehol, S and Pena, H. 2016. Distribution and abundance of Norwegian spring spawning herring during the spawning season in 2016. Survey report / Institute of Marine Research/ /ISSN 1503 6294/Nr. 17–2016
- Slotte, A., Salthaug, A., Utne, KR, Ona, E. 2017. Distribution and abundance of Norwegian spring spawning herring during the spawning season in 2017. Survey report / Institute of Marine Research/ ISSN 15036294/Nr. 8 – 2017
- Slotte A., Salthaug, A., Høines, Å., Stenevik E. K., Vatnehol, S and Ona, E. 2018. Distribution and abundance of Norwegian spring spawning herring during the spawning season in 2018. Survey report / Institute of Marine Research/ISSN 15036294/Nr. 5– 2018.
- Vikebø, F., Korosov, A., Stenevik, E.K., Husebø, Å. Slotte, A. 2012. Spatio-temporal overlap of hatching in Norwegian spring spawning herring and spring phytoplankton bloom at available spawning substrates – observational records from herring larval surveys and SeaWIFS. ICES Journal of Marine Science, 69(7): 1298-1302.

## Tables

**Table 1.** Estimated total index of abundance (TSN), total biomass (TSB) and spawning stock biomass (SSB) of Norwegian spring-spawning herring during the spawning season 13-25. February 2019.

Length (cm)	Age																			Total				
	1	2	3	4	5	6	7	8	9	10	11	12	13	14	15	16	17	18	19	Unknown	Number	Biomass	MeanW	
12-13	-	-	-	-	-	-	-	-	-	-	-	-	-	-	-	-	-	-	-	2681	2681	32	12.0	
13-14	-	-	-	-	-	-	-	-	-	-	-	-	-	-	-	-	-	-	-	-	-	-	-	
14-15	50698	-	-	-	-	-	-	-	-	-	-	-	-	-	-	-	-	-	-	-	50698	807	15.9	
15-16	47832	-	-	-	-	-	-	-	-	-	-	-	-	-	-	-	-	-	-	-	47832	939	19.6	
16-17	11038	-	-	-	-	-	-	-	-	-	-	-	-	-	-	-	-	-	-	-	11038	235	21.3	
17-18	-	-	-	-	-	-	-	-	-	-	-	-	-	-	-	-	-	-	-	-	-	-	-	
18-19	-	-	-	-	-	-	-	-	-	-	-	-	-	-	-	-	-	-	-	-	1769	1769	64	36.0
19-20	-	1769	-	-	-	-	-	-	-	-	-	-	-	-	-	-	-	-	-	-	1769	60	34.0	
20-21	-	-	-	-	-	-	-	-	-	-	-	-	-	-	-	-	-	-	-	-	3539	3539	163	46.0
21-22	-	-	5308	-	-	-	-	-	-	-	-	-	-	-	-	-	-	-	-	-	5308	319	60.0	
22-23	-	-	28738	-	-	-	-	-	-	-	-	-	-	-	-	-	-	-	-	-	28738	1881	65.5	
23-24	-	-	70719	5409	-	-	-	-	-	-	-	-	-	-	-	-	-	-	-	-	76128	5580	73.3	
24-25	-	-	88608	3599	-	-	-	-	-	-	-	-	-	-	-	-	-	-	-	-	92207	7968	86.4	
25-26	-	-	64180	31798	-	-	-	-	-	-	-	-	-	-	-	-	-	-	-	-	95978	9618	100.2	
26-27	-	-	73604	8197	-	-	-	-	-	-	-	-	-	-	-	-	-	-	-	-	81801	9365	114.5	
27-28	-	-	28356	38165	-	-	-	-	-	-	-	-	-	-	-	-	-	-	-	-	66521	8856	133.1	
28-29	-	-	-	82204	65931	14877	-	-	-	-	-	-	-	-	-	-	-	-	-	-	163012	25598	157.0	
29-30	-	-	-	60258	172562	41328	-	-	-	-	-	-	-	-	-	-	-	-	-	-	274148	50371	183.7	
30-31	-	-	-	17847	199745	416182	10868	7203	-	-	-	-	-	-	-	-	-	-	-	-	651845	137721	211.3	
31-32	-	-	-	31375	209474	1084824	171863	60323	-	-	-	-	-	-	-	-	-	-	-	-	1557859	370659	237.9	
32-33	-	-	-	12636	92998	1237598	154025	54932	2246	-	-	-	-	-	-	-	-	-	-	-	1554435	403545	259.6	
33-34	-	-	-	12878	150416	588053	282398	183675	22891	5898	-	8075	-	-	-	-	-	-	-	-	1254285	356338	284.1	
34-35	-	-	-	-	19714	224539	135829	323226	184160	170866	90854	19871	13483	-	48120	-	13797	-	-	-	1244459	387379	311.3	
35-36	-	-	-	-	6868	47869	41512	215577	313561	405496	268816	143811	514970	43578	353049	13614	32187	-	-	-	2400907	812245	338.3	
36-37	-	-	-	-	5898	-	2297	43675	114752	361122	235740	150784	779176	121072	764077	36533	101625	3238	4784	-	2724772	982660	360.6	
37-38	-	-	-	-	15516	-	-	6986	6767	72617	130412	25977	457362	30323	578281	-	83804	-	-	-	1408045	537134	381.5	
38-39	-	-	-	-	-	-	-	-	-	17760	13973	46032	79673	13758	112611	2253	13058	-	2253	-	301370	123389	409.4	
39-40	-	-	-	-	-	-	-	-	-	-	-	-	-	-	17462	-	14481	-	-	-	31943	13874	434.4	
40-41	-	-	-	-	-	-	-	-	-	-	-	-	-	-	-	-	5898	-	-	-	5898	2654	450.0	
TSN (1000)	109567	1769	359512	304367	939122	3655271	798791	895597	644377	1033758	739795	394548	1844663	208732	1873599	52400	264850	3238	7037	7988	14138984	-	-	
TSB (t)	1981	60	33475	50448	210703	932892	221570	276212	215805	355400	261755	139988	665160	75834	684486	18548	101122	1049	2708	259	-	4249454	-	
Mean L (cm)	14.9	19.0	24.7	28.6	31.1	32.0	32.9	34.1	35.1	35.6	35.9	36.0	36.3	36.3	36.4	36.1	36.7	36.5	37.0	17.3	-	-	-	
Mean W (g)	18.1	34.0	93.1	165.8	224.4	255.2	277.4	308.4	334.9	343.8	353.8	354.8	360.6	363.3	365.3	354.0	381.8	324.0	384.8	32.4	-	-	300.6	
% mature	0	0	22	89	100	100	100	100	100	100	100	100	100	100	100	100	100	100	100	100	-	-	-	
SSB (t)	0	0	7364	44833	210703	932892	221570	276212	215805	355400	261755	139988	665160	75833	684486	18548	101122	1049	2708	-	-	4215428	-	

**Table 2.** Estimated index of abundance (TSN), total biomass (TSB) and spawning stock biomass (SSB) of Norwegian spring-spawning herring by the strata covered during the spawning season 13-25. February 2019.

Age	Stratum														Total
	2	4	5	6	7	8	9	10	11	12	13	14	16	18	
1	0	0	15	26	28	11	0	0	12	1	7	0	9	0	110
2	0	0	0	0	0	0	0	0	0	0	0	0	0	0	2
3	0	0	0	0	0	8	7	12	15	0	9	0	0	308	360
4	0	0	2	4	14	27	0	41	74	2	39	0	7	95	304
5	3	16	39	82	92	59	118	167	190	9	78	0	31	56	939
6	18	124	155	260	184	317	968	803	480	22	199	0	70	54	3655
7	1	5	57	89	103	165	173	129	33	1	9	0	34	0	799
8	8	47	57	123	156	170	69	188	20	0	6	0	49	3	896
9	8	83	100	186	90	48	21	77	0	0	0	0	32	0	644
10	17	135	161	268	200	53	0	109	17	1	6	0	64	3	1034
11	2	21	198	279	80	44	0	83	0	0	0	0	33	0	740
12	5	26	85	164	31	32	0	29	10	1	3	0	10	0	395
13	38	259	296	510	333	53	7	218	10	1	8	0	113	0	1845
14	9	57	22	33	39	5	0	30	0	0	0	0	15	0	209
15	25	207	285	495	344	88	21	268	15	2	5	0	116	3	1874
16	0	0	11	15	16	2	0	3	0	0	0	0	5	0	52
17	12	57	41	71	49	2	0	10	5	0	0	0	18	0	265
18	0	0	0	0	0	0	0	3	0	0	0	0	0	0	3
19	0	0	0	0	4	2	0	0	0	0	0	0	1	0	7
TSN (millions)	146	1035	1524	2604	1764	1086	1383	2171	880	38	370	0	607	531	14139
B (1000 tons)	52	372	517	883	582	316	341	635	195	9	82	0	200	66	4249
% Mature	100	100	100	100	100	99	100	99	98	100	99	0	100	48	98
SSB (1000 tons)	52	372	517	883	581	314	341	631	191	9	80	0	200	32	4153

**Table 3.** Uncertainty estimates in the abundance index of Norwegian spring-spawning herring during the spawning season 13 -25 February 2019. Uncertainty estimates are from 500 bootstrap replicates in StoX. See also Figure 10 for graphical presentation of data.

Age	5th percentile	Median	95th percentile	Mean	SD	CV
1	0.0	90.9	189.2	80.7	69.5	0.86
2	0.0	1.7	5.0	1.9	1.7	0.91
3	119.8	353.4	745.8	377.1	188.3	0.50
4	216.7	304.1	415.2	309.3	61.3	0.20
5	701.1	917.5	1207.0	932.3	149.9	0.16
6	2594.7	3746.4	5010.1	3752.7	761.7	0.20
7	506.1	730.2	1051.1	749.9	169.5	0.23
8	716.2	883.8	1071.5	883.2	106.9	0.12
9	479.7	646.9	884.9	660.9	125.0	0.19
10	846.6	1048.7	1313.3	1060.8	143.1	0.13
11	549.0	732.5	985.8	747.6	133.9	0.18
12	290.4	406.0	570.6	416.2	88.1	0.21
13	1385.5	1790.1	2425.6	1836.6	324.1	0.18
14	104.9	178.6	276.1	182.8	53.1	0.29
15	1428.8	1811.6	2298.6	1838.5	266.1	0.14
16	7.2	48.3	91.2	48.7	24.8	0.51
17	174.4	273.3	415.3	281.9	72.9	0.26
18	0.0	4.4	18.9	5.8	6.4	1.11
19	0.0	8.4	18.8	8.4	6.3	0.76

## Figures

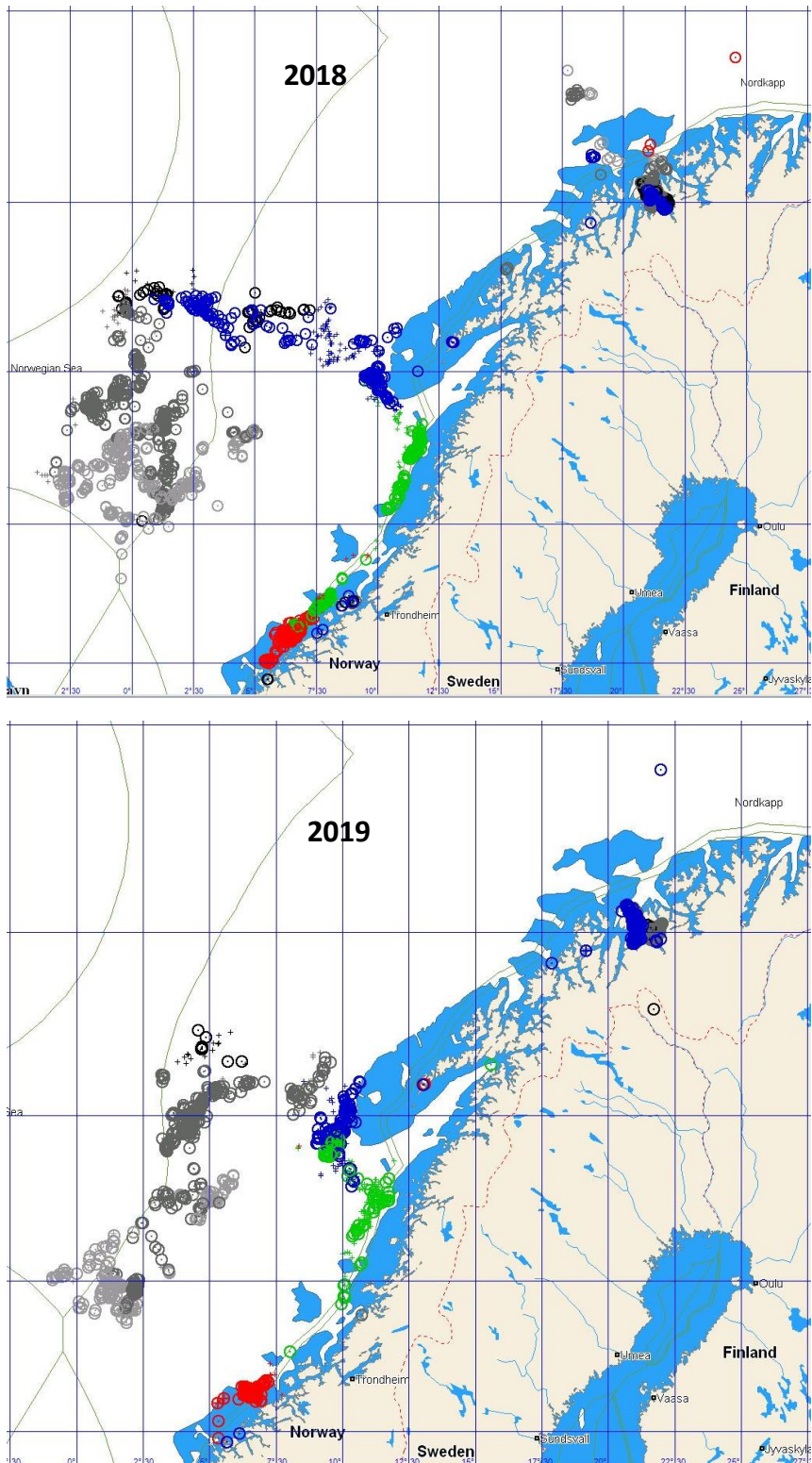


Figure 1. Monthly distribution of catches of Norwegian Spring spawning herring from October until February, based on electronic logbooks. Each point represent one catch, only catches larger then 5 tonnes are shown. Small crosses=trawl catches, circles (with dot inside)=purse seine, light grey=October, dark grey=November, black=December, blue=January, green=February 1-12, red=February 13-28 (overlapping with survey period).

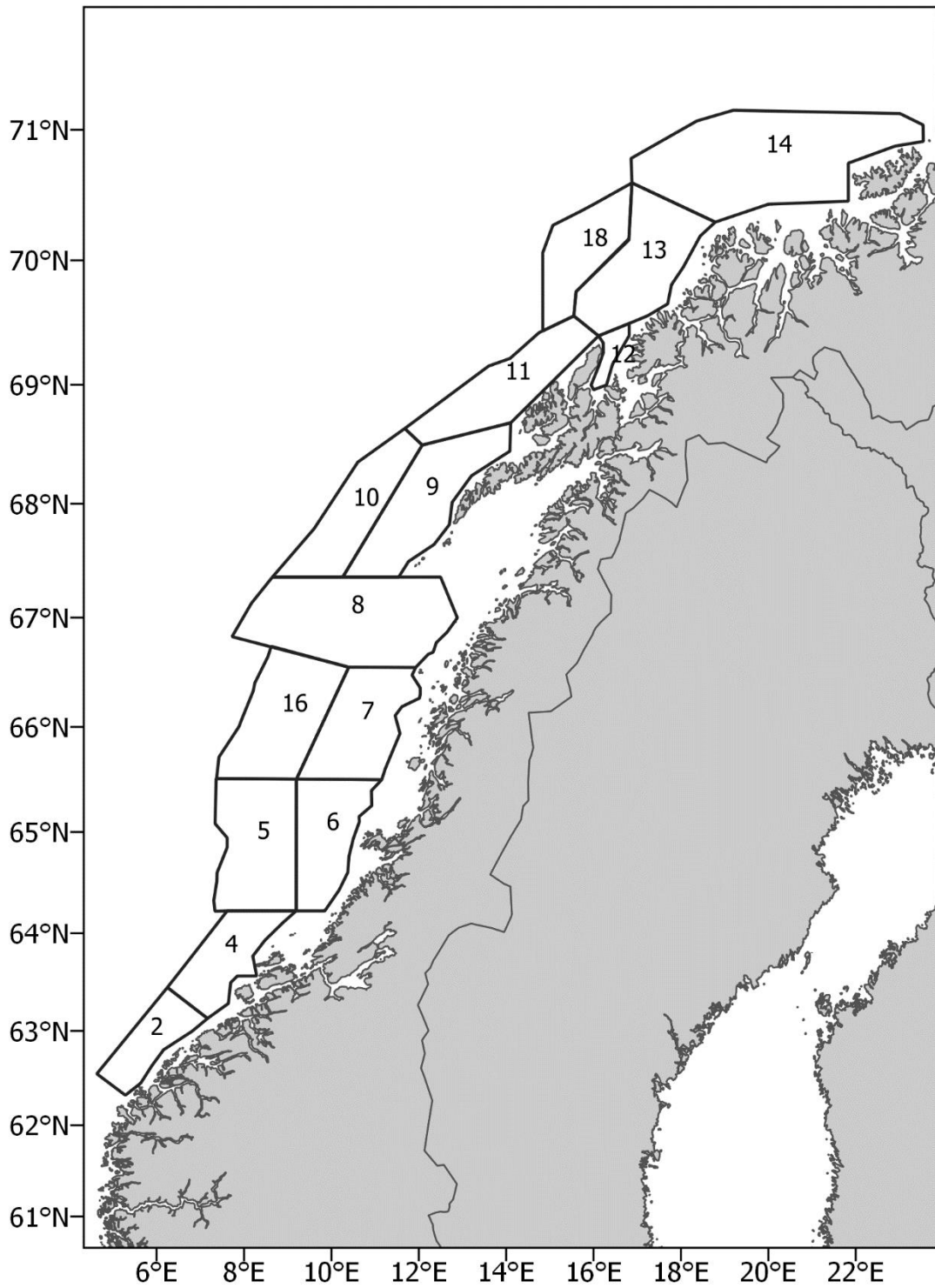


Figure 2. Strata covered during 13-25. February 2019 with MS *Eros*, *Kings Bay* and *Vendla*

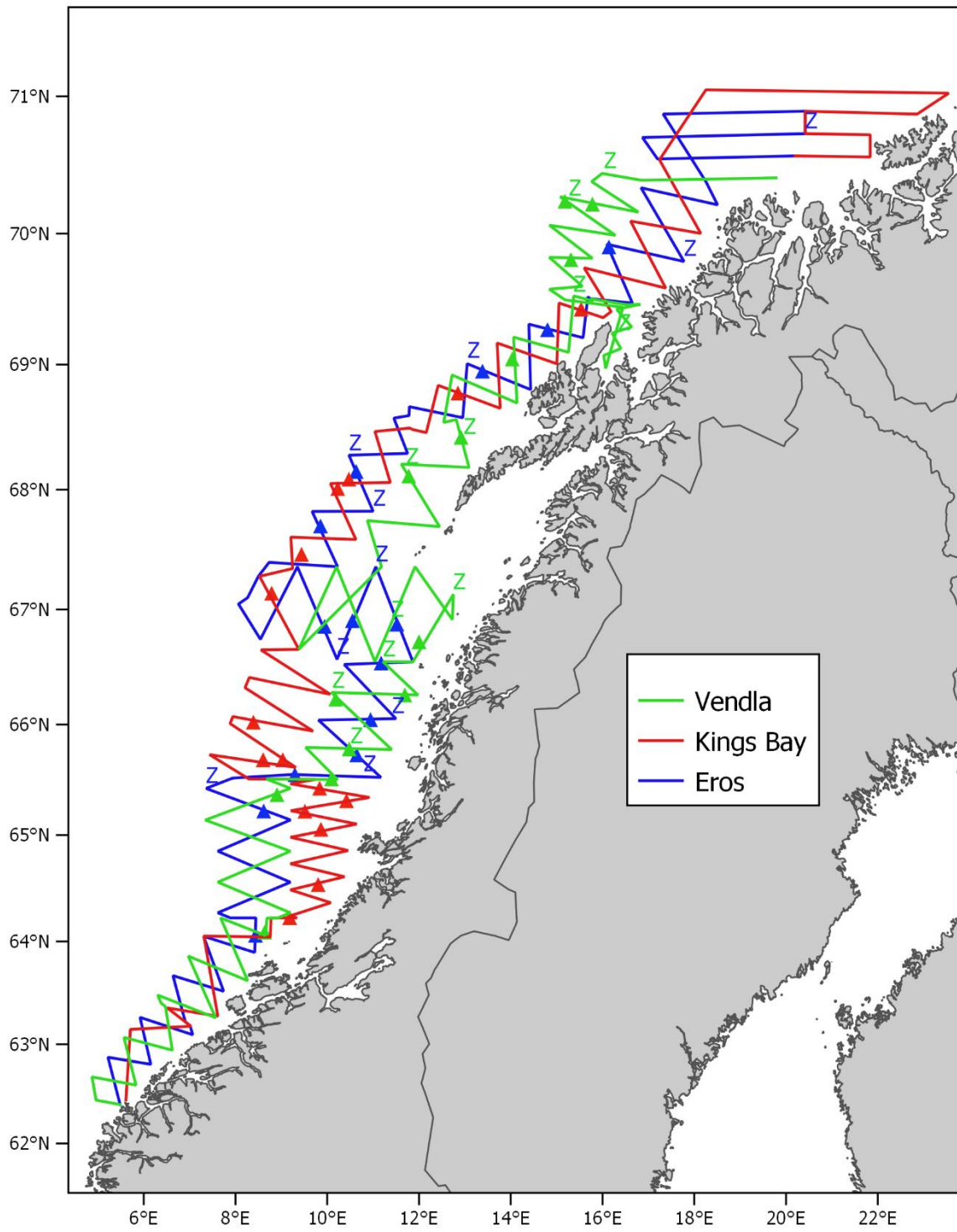


Figure. 3. Acoustic transects, pelagic trawl stations (triangles), and CTD stations (Z) covered with *Eros*, *Kings Bay* and *Vendla* 13-25 February 2019.

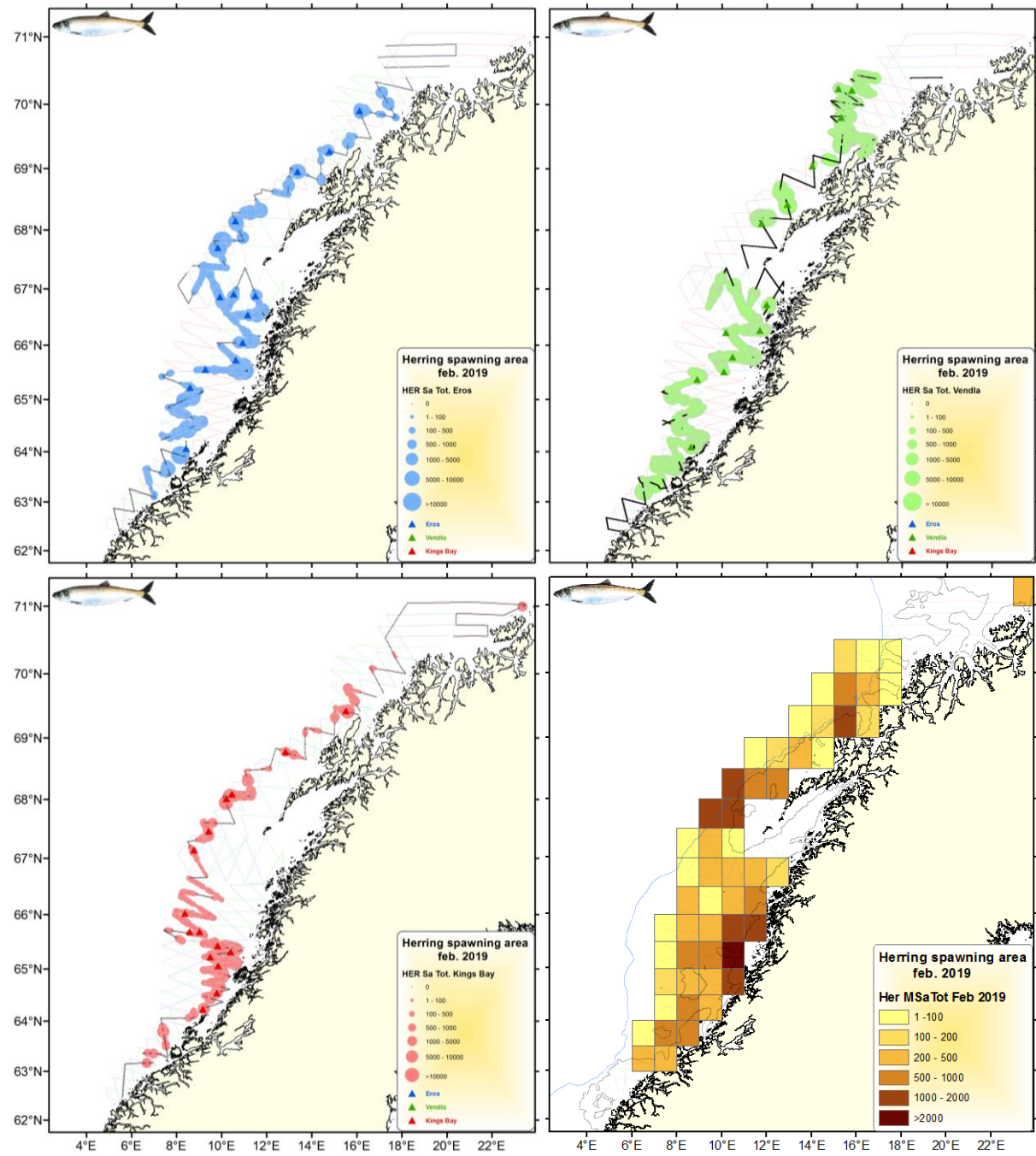


Figure 4. Acoustic density (NASC) of herring recorded during 13-25. February 2019. Bubbles represent 0.1 nm NASC values shown per vessels (*Eros*, *Kings Bay* and *Vendla*). Also shown is mean NASC within geographical rectangles using data from all vessels (bottom right). See Annex 5 for examples of acoustic registrations in the survey area from *Kings Bay*.

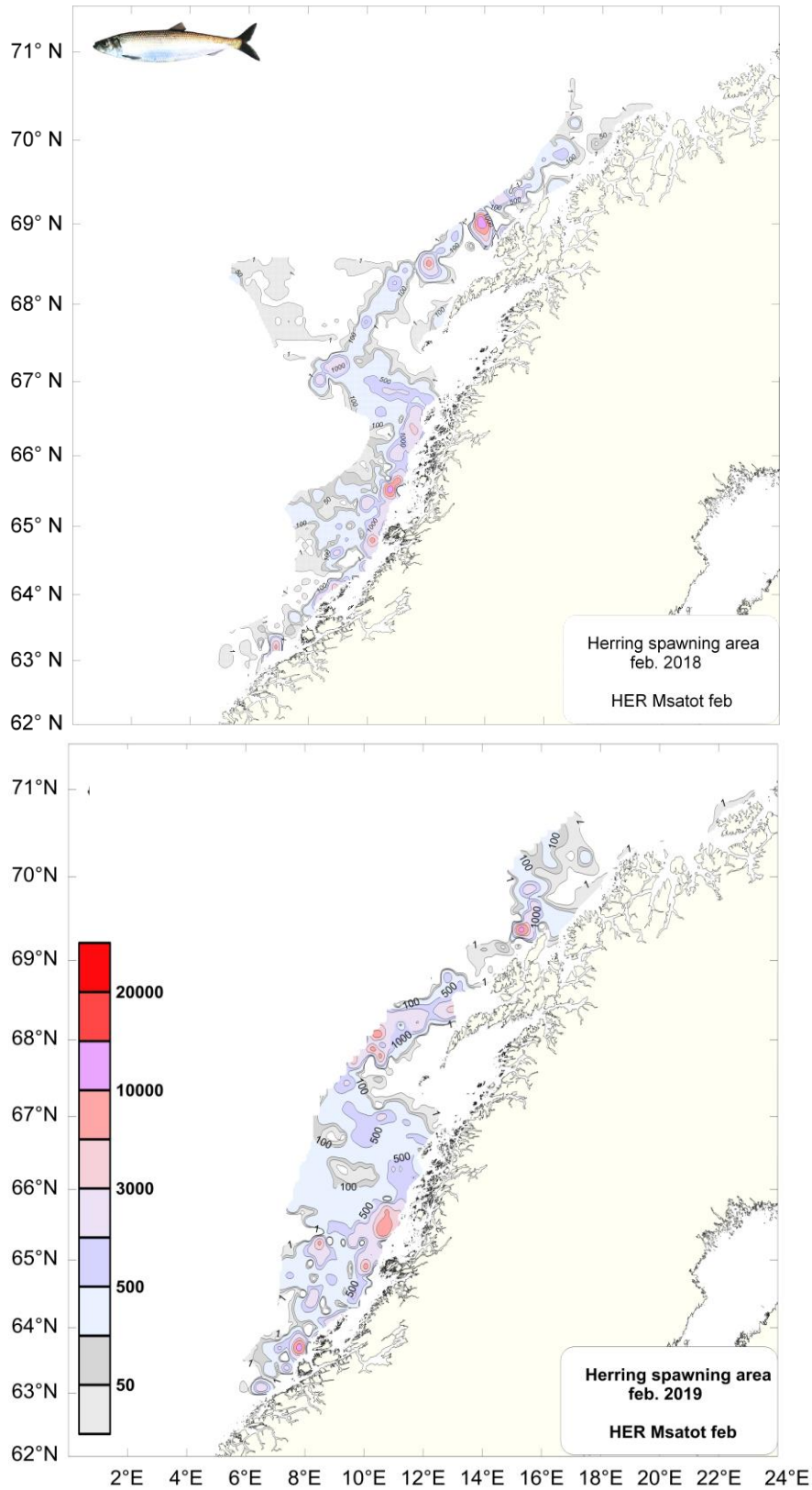


Figure 5. Distribution and acoustic densities (NASC) of herring recorded during 13-25. February 2019 (bottom), compared with the situations in 2018 (top).

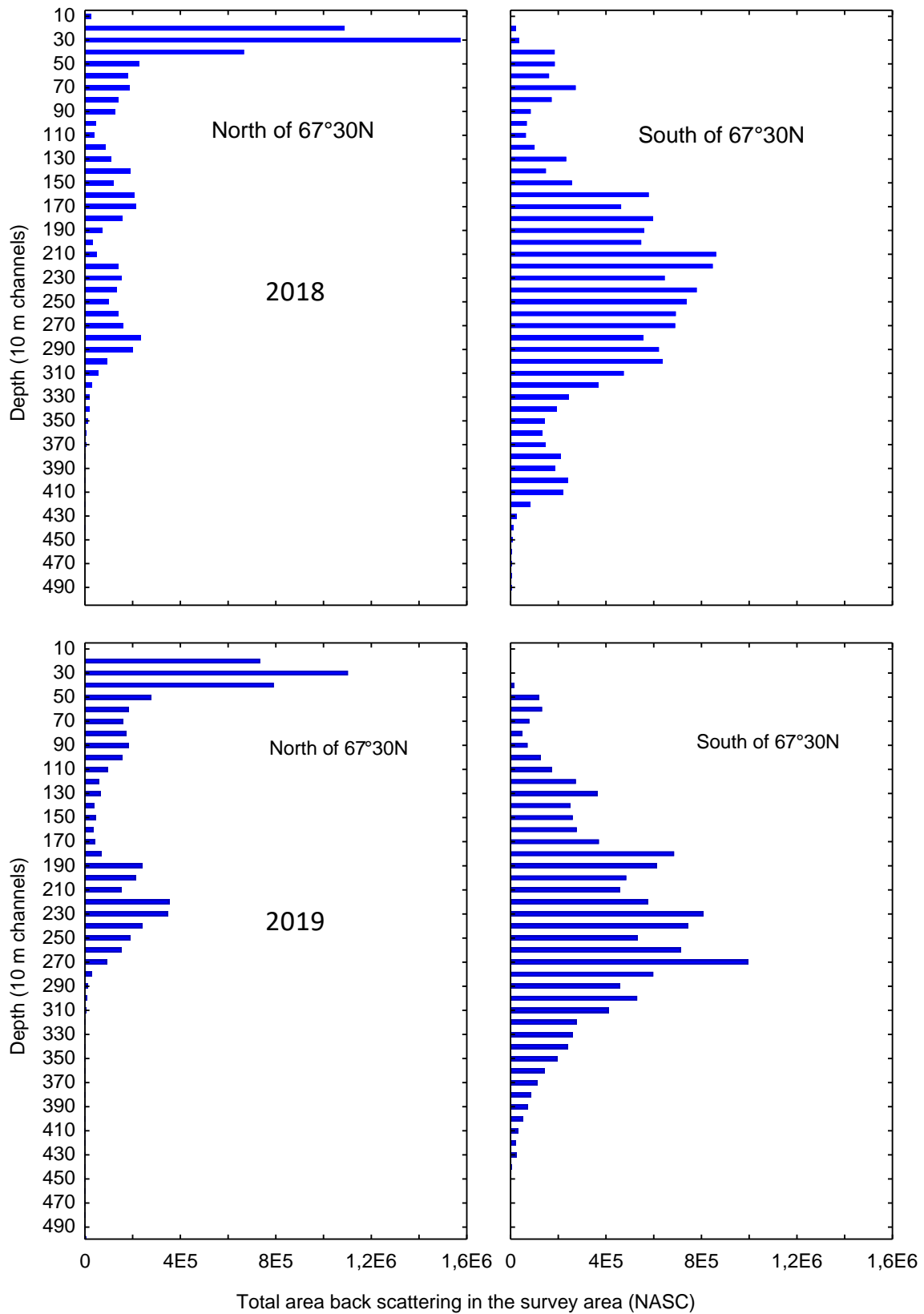


Figure 6. Total acoustic back scattering (NASC) by 10 m depth channels in the survey area during 13-25 February. Comparison between areas to the south and north of 67°N, and between the surveys in 2018 and 2019.

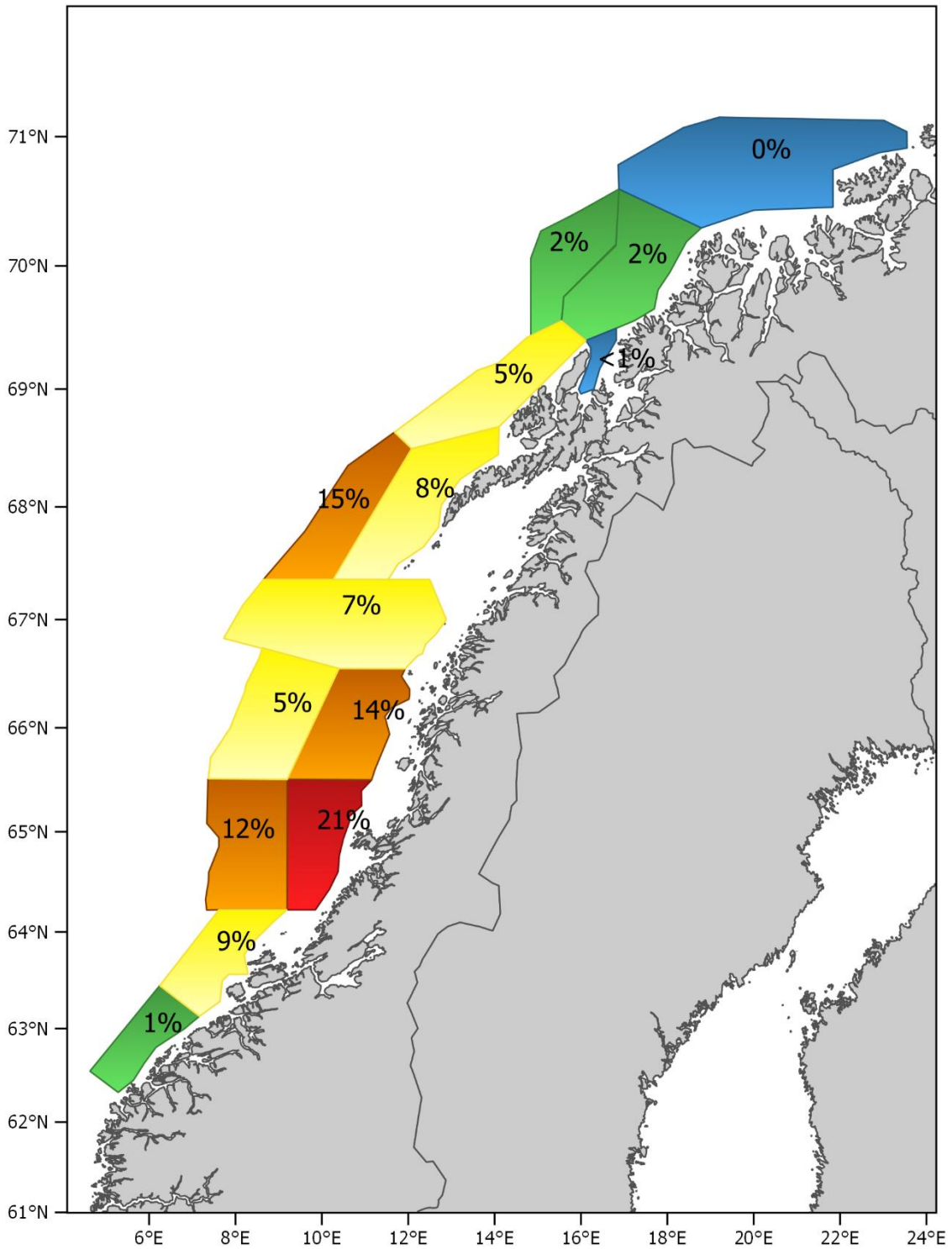


Figure. 7. Relative (%) distribution of the estimated biomass of herring between the strata covered by *Eros*, *Kings Bay* and *Vendla* 13-25 February 2019. See Table 3 for details on the estimates from each strata.

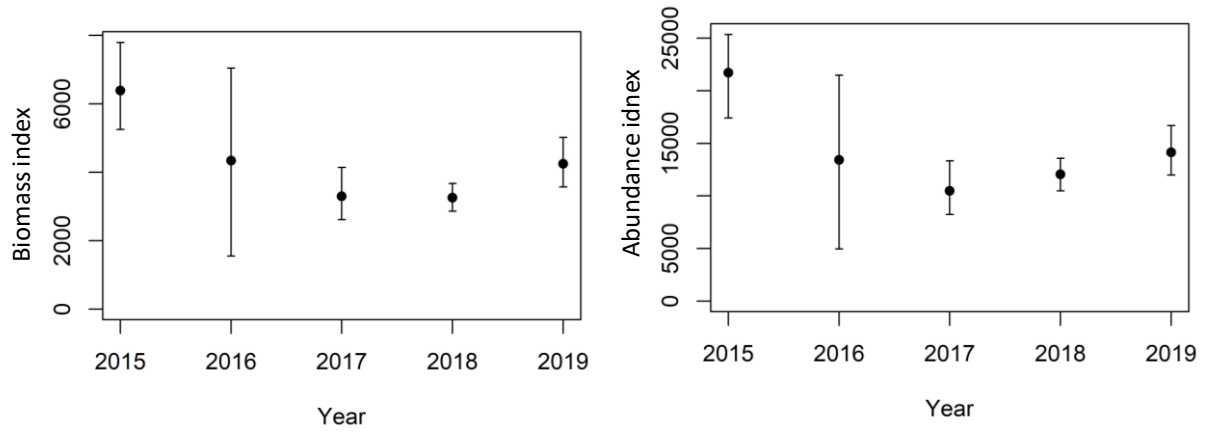


Figure 8. Index of total biomass and abundance estimated from the Norwegian spring-spawning herring spawning surveys 2015-2019 (the error bars represent 90% confidence intervals).

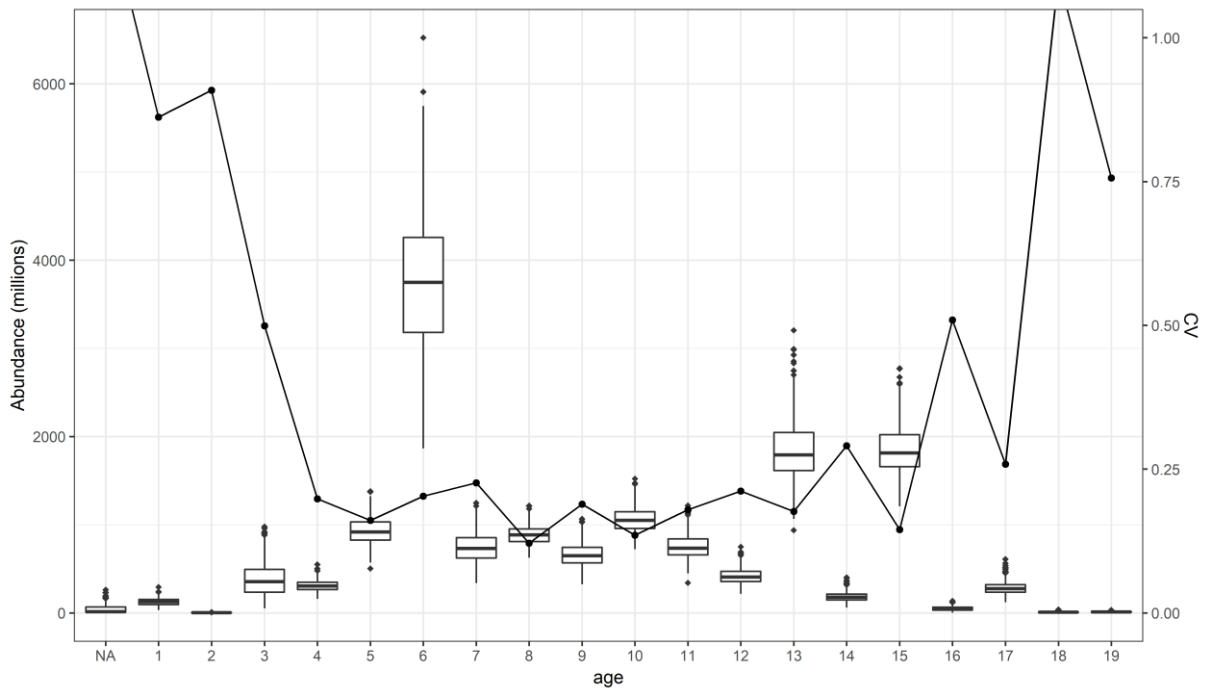


Figure 9. Standard box plot of abundance index by age with uncertainty as estimated during 13-25 February 2019. The Uncertainty estimates were based on 500 bootstrap replicates in StoX. See Table 2 for details on the data presented.

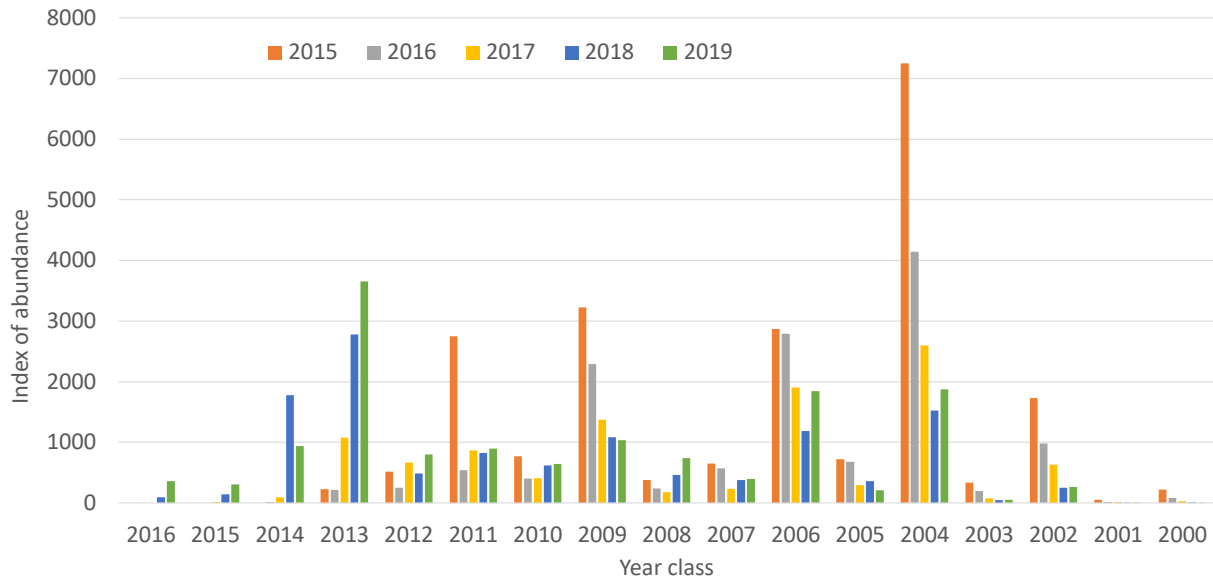


Figure 10. Abundance index by year class estimated during the Norwegian spring-spawning herring surveys 2015-2019.

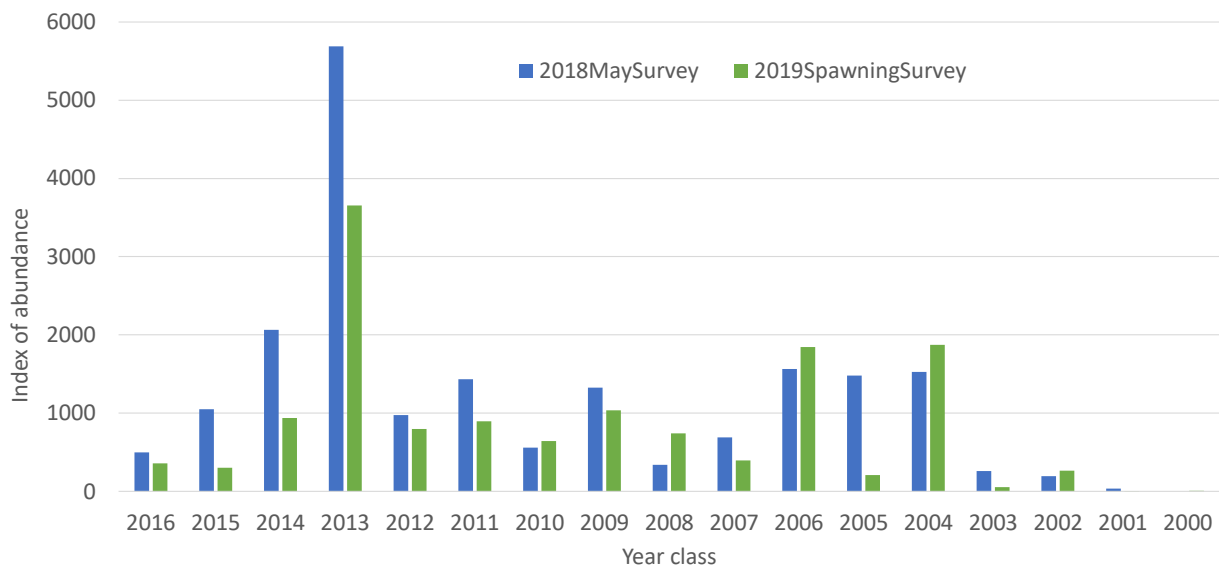


Figure 11. Comparison of abundance index by year class between the Norwegian spring-spawning herring survey 2019 with the index from the international ecosystem survey in the Norwegian Sea in May 2018 (IESNS).

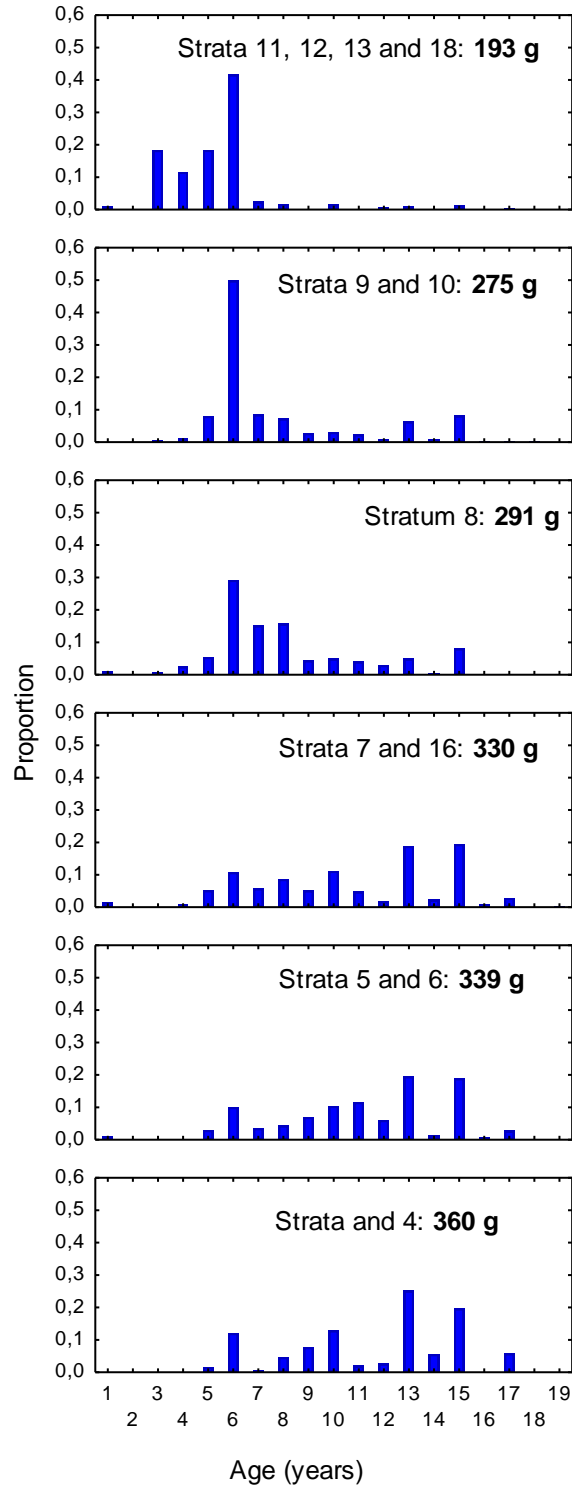


Figure 12. Comparison of age composition (%) and mean weight (bold) estimated in different strata covered during 13-25. February 2019. Se Figure 1 for spatial distribution of strata.

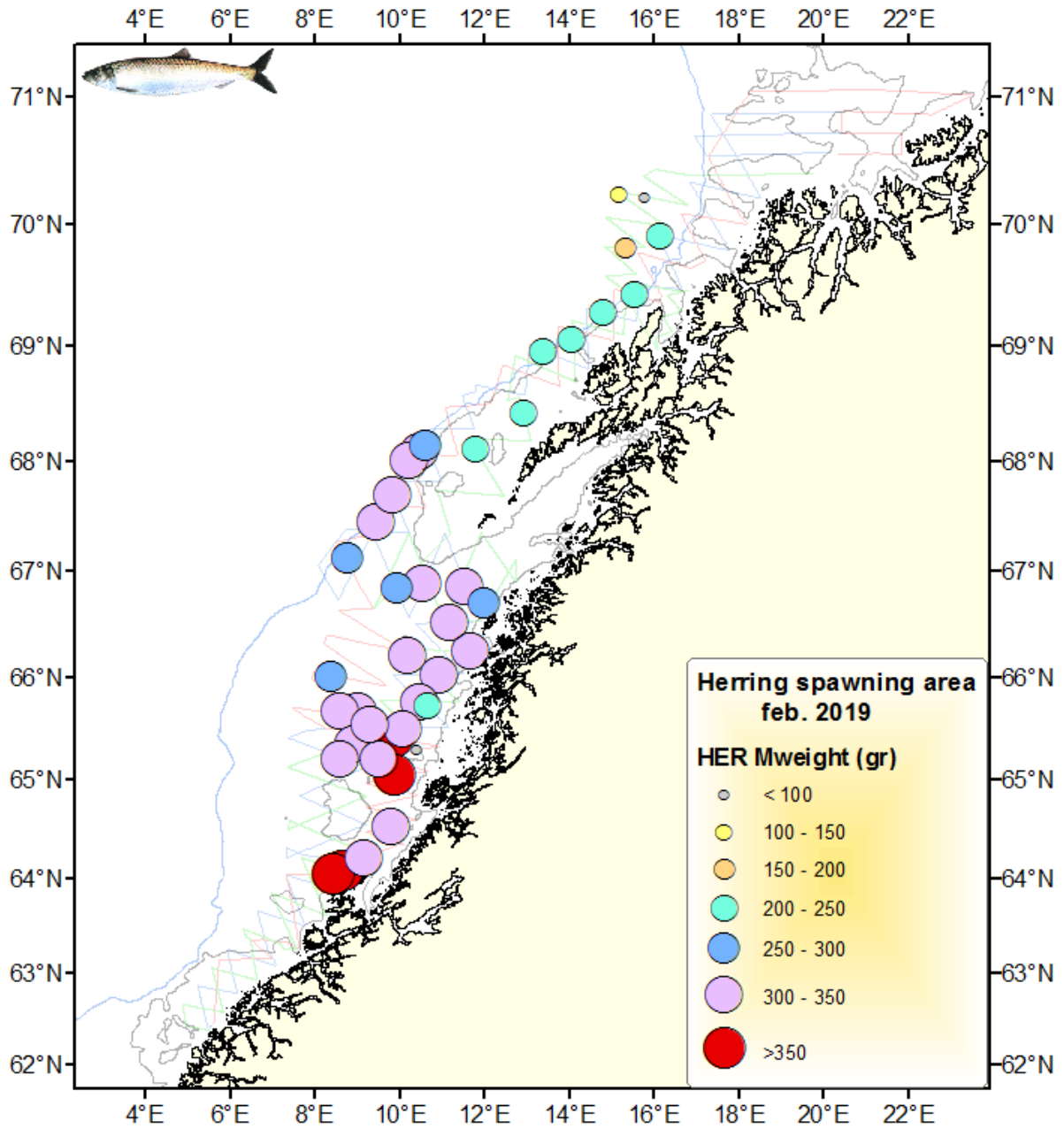


Figure 13. Spatial differences in mean herring weight (g) during the Norwegian spring-spawning herring survey13-25. February 2019.

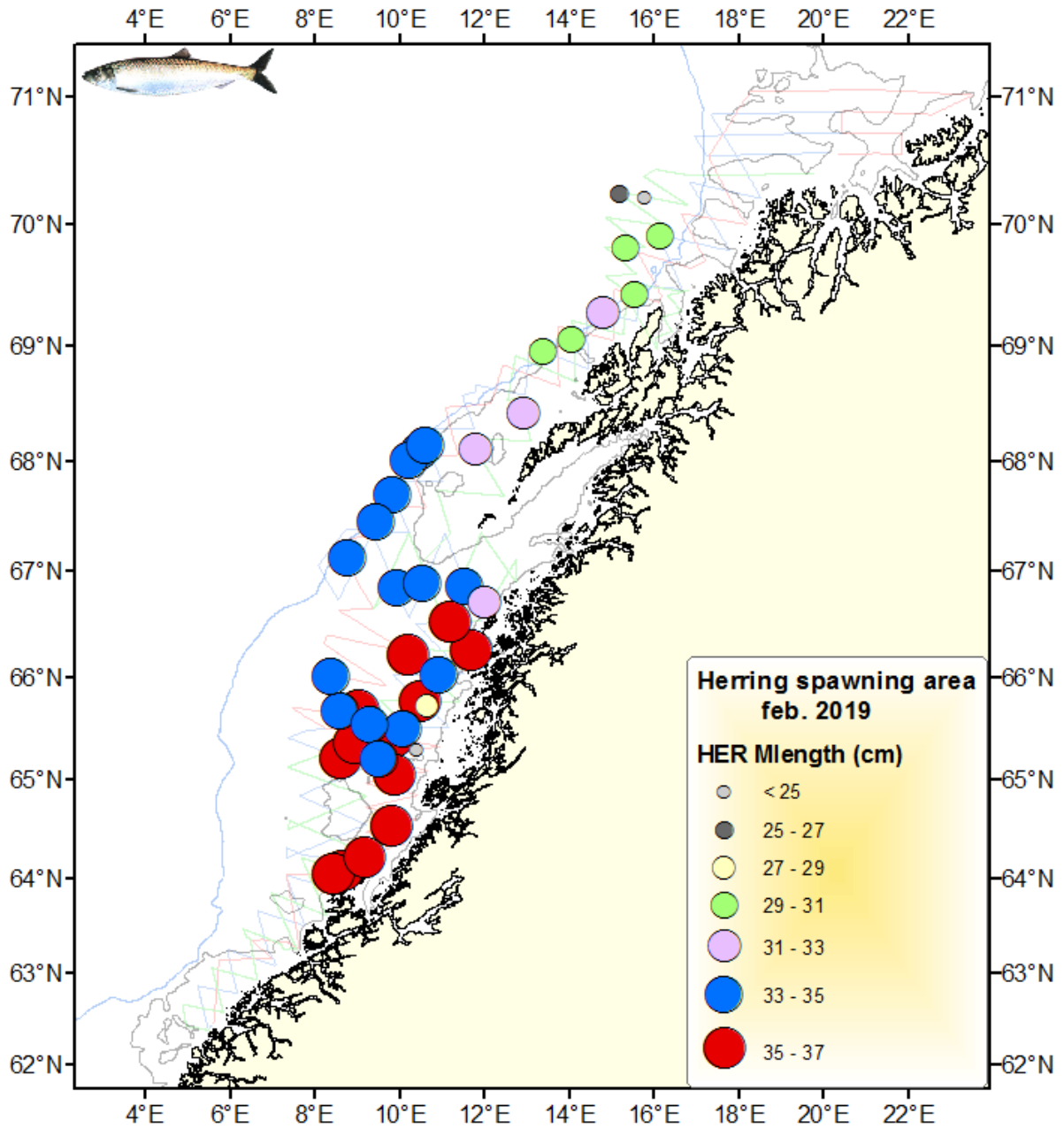


Figure 14. Spatial differences in mean herring body length (cm) during the Norwegian spring-spawning herring survey 13-25. February 2019.

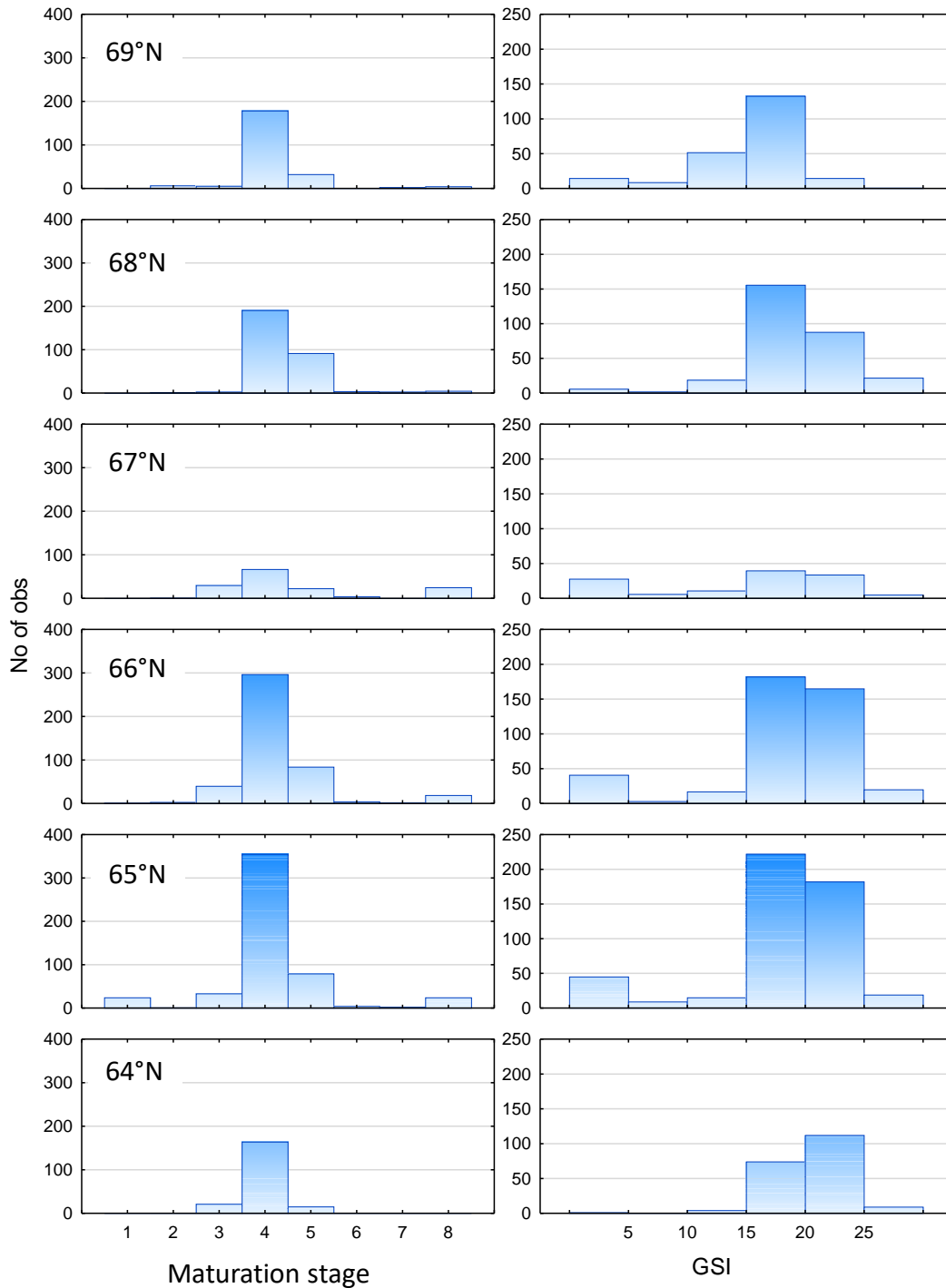


Figure 15. Latitudinal variation in maturation during the Norwegian spring-spawning herring survey13-25.February 2019. Data are not weighted by acoustics, simply frequency of fish analysed. Shown is maturation stage on a subjective scale, where 1-2= immature, 3=early maturing, 4=late maturing, 5=ripe, 6=spawning, 7=spent, 8=resting stages, as well as GSI (gonadosomatic index; % gonad weight relative to total weight).

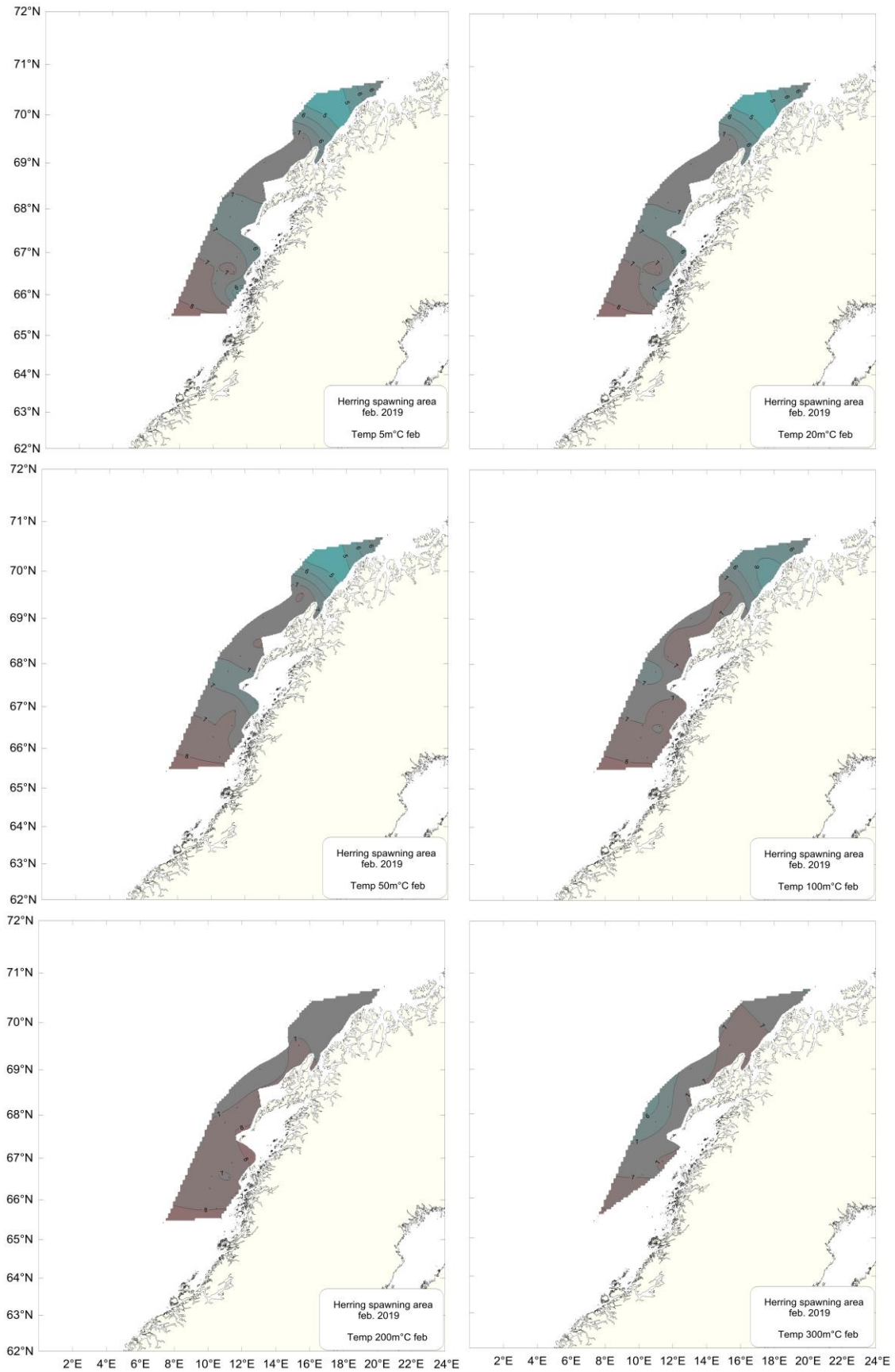


Figure 16. Temperature at 5, 20, 50, 100, 200, 300 m in the area covered during the Norwegian spring-spawning herring survey 13-25. February 2019.

## Annex 1. Calibration results and settings

Table 1. Calibration data and parameter settings of the five Simrad EK80 WBT's the five EK60 GPT split-beam echo sounders mounted on respectively on Kings Bay, Vendla and Eros as used during the survey. The new WC57.2 calibration sphere was as target for all frequencies when calibration at the fishery pier in Ålesund, with tabulated values for the sphere TS on EK60, and with the internally computed by the calibration program in EK80. An error in the calibration program of the EK80 at 18 and 38 kHz was discovered during the survey in 2017 and corrected for in postprocessing. The error was corrected in the EK80 software version 1.12.2. For the two other vessels, using Simrad EK60, the calibration data below was used, as measured in Aalesund February 13. 2018. The validity of the WC 57.2 calibration sphere against the CU60 was previously done on G.O.Sars in November 2018 with good results. The echo sounders calibration showed very good stability compared to 2017, while the 200 kHz transducer on Kings Bay was defect and not used.

MS Kings Bay, Simrad EK80					
Parameter	Survey data sample 20190213 02: Simrad EK80, narrow-band				
Transducer type	ES18	ES38B	ES70-7C	ES120-7C	ES200-7C
Transmission frequency [kHz]	18	38	70	120	200
Transmission power [W]	2000	2000	750	250	150
Pulse duration [ms]	1.024	1.024	1.024	1.024	1.024
TS Transducer Gain [dB]	23.04	23.9	27.77	26.91	Defect (not used)
Sa Correction (dB)	0.001	0.005	0.13	0.08	
Equivalent beam angle [dB]	-17.0	-20.7	-20.7	-20.7	-20.7
Absorption coefficient [dB km <sup>-1</sup> ]	2.9	10.1	20.9	31.8	52.15
Half power beam widths (along/athwart ship) [deg]	11.08/9.7 7	7.1/7.23	6.7/6.72	6.34/6.46	6.67/6.43
Transducer angle sensitivity (along ship and athwart ship)	15.5	23.0	23.0	23.0	23.0
Sound speed [m s <sup>-1</sup> ]	1475	1475	1475	1475	1474

M/S Vendla, Simrad EK60					
Parameter	Calibration 20190218 Simrad EK60, CW narrow-band				
Transducer type	ES18	ES38B	ES70-7C	ES120-7C	ES200-7C
Transmission frequency [kHz]	18	38	70	120	200
Transmission power [W]	2000	2000	750	250	120
Pulse duration [ms]	1.024	1.024	1.024	1.024	1.024
TS Transducer Gain [dB]	22.83	25.58	26.51	27.18	27.48
Sa Correction (dB)	-0.57	-0.66	-0.31	-0.32	-0.26
Equivalent beam angle [dB]	-17.0	-20.6	-20.7	-21.0	-20.7
Absorption coefficient [dB km <sup>-1</sup> ]	2.8	9.6	20.3	31.3	44.5
Half power beam widths (along/athwart ship) [deg]	10.61/10. 88	7.15/7.04	6.61/6.59	6.44/6.56	6.27/6.21
Transducer angle sensitivity (along ship and athwart ship)	15.5	23.0	23.0	23.0	23.0
Sound speed [m s <sup>-1</sup> ]	1475	1475	1475	1475	1475

M/S EROS, Simrad EK60					
Parameter	Calibration 20180218, Simrad EK60, CW narrow-band				
Transducer type	ES18	ES38B	ES70-7C	ES120-7C	ES200-7C
Transmission frequency [kHz]	18	38	70	120	200
Transmission power [W]	2000	2000	375	150	90
Pulse duration [ms]	1.024	1.024	1.024	1.024	1.024
TS Transducer Gain [dB]	22.13	26.05	26.86	26.61	25.98
SaCorrection [dB]	-0.78	-0.66	-0.36	-0.31	-0.30
Equivalent beam angle [dB]	-17.0	-20.6	-20.7	-21.0	-20.7
Absorption coefficient [dB km <sup>-1</sup> ]	2.8	9.7	20.6	31.6	44.9
Half power beam widths (along/athwart ship) [deg]	10.98/10. 80	7.04/6.90	6.61/6.60	6.46/6.51	6.41/6.22
Transducer angle sensitivity (along ship and athwart ship)	15.5	23.0	23.0	23.0	23.0
Sound speed [m s <sup>-1</sup> ]	1475	1475	1475	1475	1474

## **Annex 2. Sonar report**

By Sindre Vatnehol

### **Purpose for using sonar**

Fish in the echo sounder's blind zone and avoidance behaviour of fish, caused by the presence of the vessel, are often referred to as potential sources of bias when developing annual indices (Løland et al. 2007). Horizontally observing equipment, such as scientific and fisheries sonars, may have the potential to measure the presence and magnitude of these measurement biases and if these have changed between years/areas. Data from calibrated fisheries sonars have been collected from all participating vessels since 2015. Methods to quantify or evaluate the extend of these biases are presently being developed.

### **Sonar preparation:**

The low-frequency sonars, either the Simrad SX90 or the Simrad SU90, were not calibrated as these have already been calibrated on other surveys. Given the considerable size of the data stream from 64 beams, all sonar data was stored directly to a 2TB external hard drive. Backup was daily made by IMR's personnel on each vessel.

We used the same sonar setting that has been used since 2015.

- The horizontal beam fan was slightly tilted to 8 degree below the horizon (Horizontal mode)
- For vertical mode, the fan of beams was set to observe perpendicular to the vessel's heading direction.
- Frequency of 30 kHz
- Range of 600 meter
- Noise-filter was switched off as this filter corrupts the data.

## Visual interpretation of the data

Methods for evaluating the extension of the biases are still being developed; hence, no temporarily estimates will be presented here. However, some remarks of what was observed is made.

For most of the transects, most of the fish were observed by the echo-sounder to be close to the seabed, hence not within the sonar detection volume.

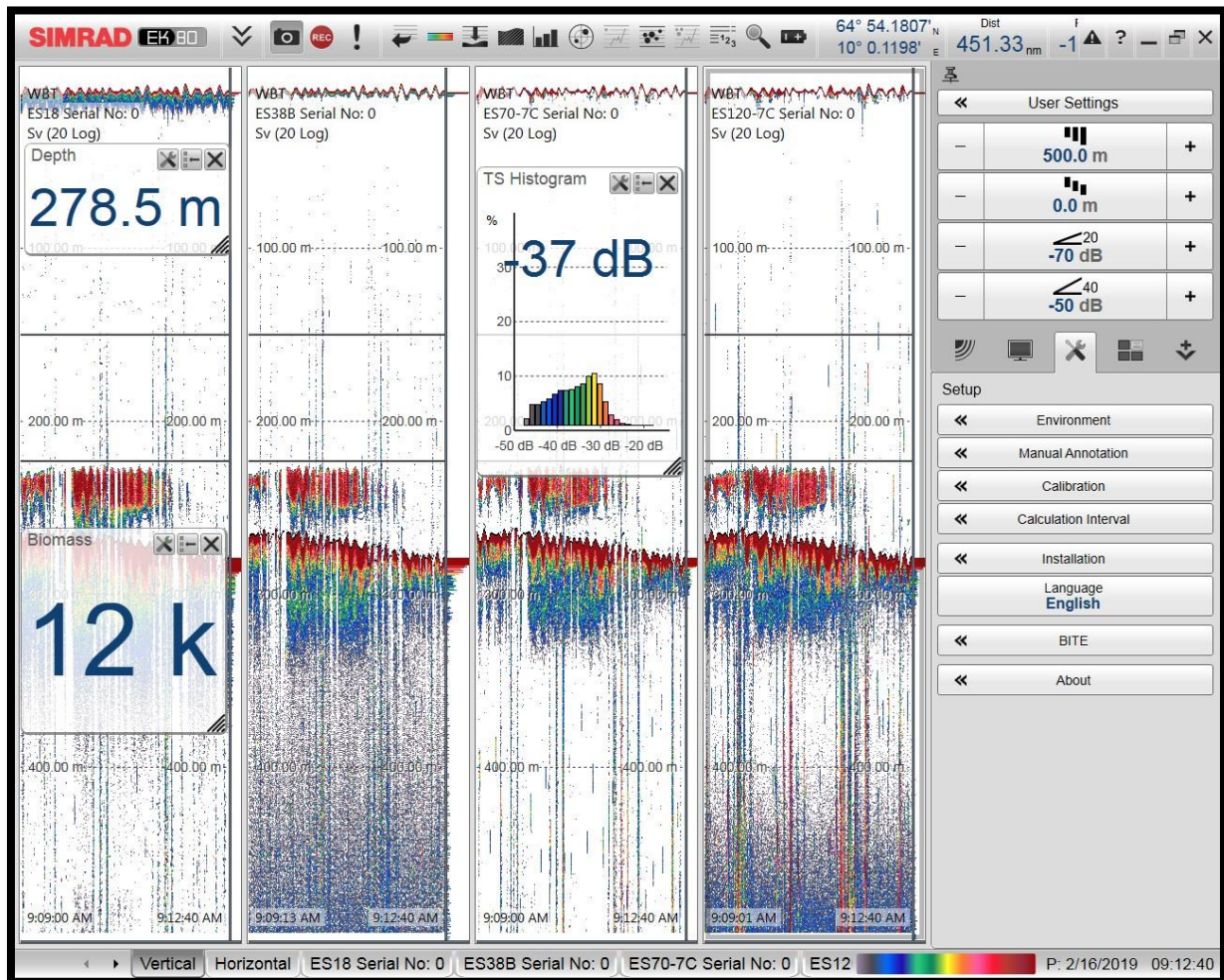
In the northern strata the fish was distributed closer to the sea surface and was thus also recorded by the sonar. Some of these registrations originated from relatively young herring.

## References:

- Cutter, George R., and David A. Demer. 2007. "Accounting for Scattering Directivity and Fish Behaviour in Multibeam-Echosounder Surveys." *ICES Journal of Marine Science* 64 (9): 1664–74. doi:10.1093/icesjms/fsm151.
- Løland, Anders, Magne Aldrin, Egil Ona, Vidar Hjellvik, and Jens Christian Holst. 2007. "Estimating and Decomposing Total Uncertainty for Survey-Based Abundance Estimates of Norwegian Spring-Spawning Herring." *ICES Journal of Marine Science* 64 (7): 1302–12. doi:10.1093/icesjms/fsm116.

### Annex 3. Corrections for air bubble attenuation on keel-mounted echo sounders

By  
Egil Ona IMR



Air bubble sound attenuation in fisheries acoustic surveys is a well-known problem (Urlick, 1967; Dalen and Hovem, 1981), while the main portion of the problem was solved by mounting transducers on a drop keel (Ona & Traynor, 1990), extending up to 3 meters below the hull of the vessel. In very strong wind and wave conditions, however, also bubble attenuation may occur on keel mounted systems. The three fishing vessels used in the survey had nearly identical echo sounder equipment during the survey, with very similar ship design and transducer mountings, all on drop keels.

Several Simrad split beam transducer were mounted in a close packing arrangement (Fig 1.), and all vessels were using the keel in maximum extension, 2.85 m outside the vessel hull. The transducers where was installed with a draft of 8.5 meters, making a large difference in attenuation compared to hull mounted systems (see Novarani & Bruno 1982).



*Figure 1. Drop keel system of the fishing vessels used. (Example)*

In very bad weather, especially with little or no herring registrations in the survey area, we adopted a procedure for air bubble attenuation like the one suggested for 38 kHz by Shabangu et al, (2014), using F/F Kings Bay as the reference vessel. Integrated backscattering from the air bubble layer in front of the transducer was used as an index for air bubble attenuation, which previously have been found to be a good proxy, and well correlated with the air bubble attenuation (Ona, 1991; Ona & Traynor 1990). A permanent integrator layer from 5 m in front of the transducer, well out of the transducer ringing zone, and outside the transducer near field, to about 25 meters were used as a scaling factor. Two factors are then estimated and corrected for;

1. Constant and variable air bubble layers brought down with wind, waves and vessel
2. Lost transmission power, blocking, or reception, appearing as or “white” pings in the echogram.

Earlier investigations have used either the number of lost pings as a proxy, or the frequency of “bad” or weak bottom echo returns.

If the post processing system are reporting these, or are systematically removing pings with blocking, like the IMR ND10 integrator, used before 1990, (See Blindheim et al., 1981; Ona & Mamylov 1988), the correction factors for air bubble attenuation will be lower, then needing to only correct for the air bubble layer itself. The comparison to the Soviet echo integrator system revealed this difference in the 1970-1990 cooperative Barents Sea surveys. Modern echo integrators, like LSSS and others, does presently not measure the fraction of weak or lost pings, and this correction may therefore be of the same order as for the air bubble attenuation alone.

The magnitude of this dropouts has been tried estimated with special experiments where the vessel first is going into the waves, measuring dropouts, and then turning with the wind and measuring the difference in backscattering of the bottom echo. Monitoring of the vessel heave, pitch and roll were also conducted during these experiments.

Especially vessel pitch, where the bulb of the vessel is pulled out of the water, and then knocked down through the waves again, seemed to cause deep air bubble clouds, as earlier documented with camera on the drop keel of G.O.Sars by Knudsen (2012).

Comparative measurements against the backscattering from the bottom echo over some nautical miles with and without air bubble attenuation will then give estimates for the total attenuation, or data for establishing a correction factor, just like applied in a more sophisticated comparative manner with two multiplexed transducers in Shabangu et al, (2014). On two transects in the

present survey, F/F Kings Bay sailed first against the wind and waves, and then returned on the same transect with the wind and waves, with practically no air bubble attenuation. Data from these comparisons of the bottom echo backscattering, averaged over 1 nautical mile bins are shown in Figure 1. The wind speed was measured by the weather station onboard, and the vessel speed subtracted by the Olex system, giving real wind speed and direction. The wave height was not recorded scientifically, but visually estimated by the captain, while the vessel movement was logged to the echo sounder raw files for each ping.

In really bad weather conditions, at  $30 - 35 \text{ ms}^{-1}$  wind speed and 7-8 meter waves, the nautical area scattering coefficient, NASC, in the air bubble layer exceed  $1000 \text{ m}^2\text{nmi}^{-2}$ , and the backscattering from the bottom was 50% lower compared to the backscattering when sailing in opposite direction. Successive data on two transects were used to establish the curve, using the shape indicated in Shabangu et al. (2014), fitting the data to a  $y=c+ a*x^b$  relationship, nonlinear regression methods, yielding parameter estimates for c, a and b, with asymptotic estimates for the parameter standard deviations, and confidence intervals for the parameter estimates.

It is suggested that the correction factor is realized in a stepwise manner, like indicated in Fig.2

## Suggested implementation 2019

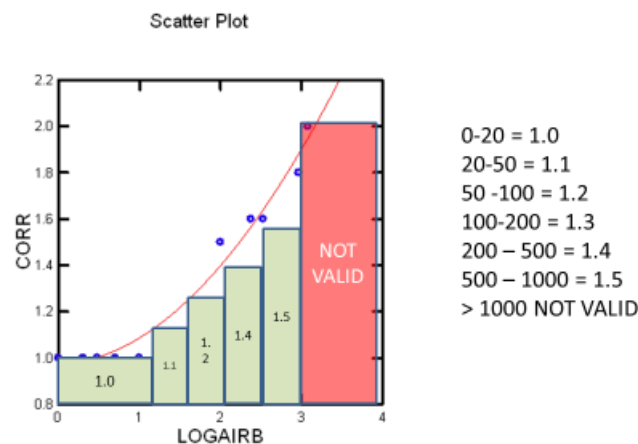


Figure 2. Suggested correction curve for air bubble attenuation during the herring survey February 2019, realized in stepwise manner, using Table to the right for the figure.

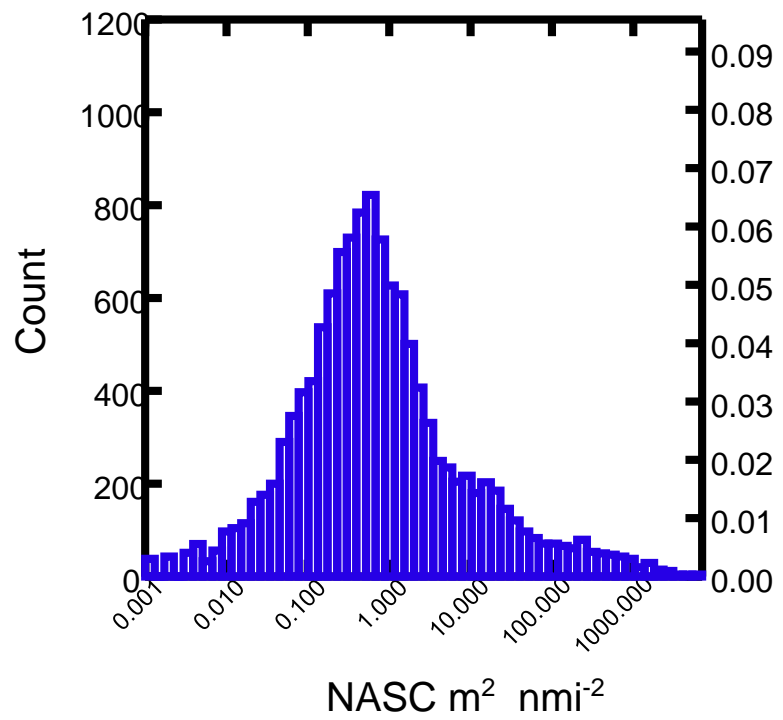
Procedure during interpretations.

1. Estimate the indicator for air bubble attenuation = Mean NASC for layer 5 – 25 meters, being sure that no pings from transmit pulse goes into the layer.
2. Scrutinize like normal, isolating herring aggregations on echogram and allocate the NASC to herring.

3. Move the air bubble correction button for the whole 5 nmi section to for example 1.2 if you want to correct the entire file, and pull the allocation percentage to full scale 120%, which now is possible.
4. Similarly, if you will correct only for LOST PINGS:
  - a. Evaluate the % of lost pings visually, by inspecting the integrator line, and then evaluate how much of the concentration which have been lost by lost pings.
  - b. Use the MAXIMUM ALLOCATION BUTTON under the air bubble correction factor button in the interpretation window, and scale the NASC to the correct value, for example 20% = 1.2, WHEN YOU NOW CAN ALLOCATE MORE THAN 100% OF THE MEASURED VALUE.
5. In the case of lost pings, at least for Kings Bay, there is sometimes one single noise stripe, following one or several lost pings. This noise probably comes from the propeller cavitation when the propeller lose pressure when the bow is going down into a wave.
6. The backscattering from this noise stripes sometimes compensates for the lost pings, and less correction may then be given. Detailed inspection of this phenomena may be studies in the data but was not prioritized here. The correlation between wind speed, heave, roll and especially pitch and this phenomenon was, however clear.

The accuracy of the correction is evaluated to be  $\pm 10\%$  when using corrections below 1.5, and the most applied correction in the start of the survey with low densities of herring was 1.1 and 1.2. Even if the weather was quite rough in the start of the survey, the extra uncertainty will disappear in the total uncertainty, as relatively low fraction of the data is corrected for air bubble attenuation. The probability density function for measured NASC for the observations made before February 22 is shown in Fig. 3.

Figure 3. Air bubble NASC in the upper layer from 5 to 25 m for the survey between 13. February and 22 February, using ESU of 0.1 nmi. The data where air bubble attenuation was applied is from 10 to 1000 in this figure. As apparent, only a fraction of the data has been corrected.



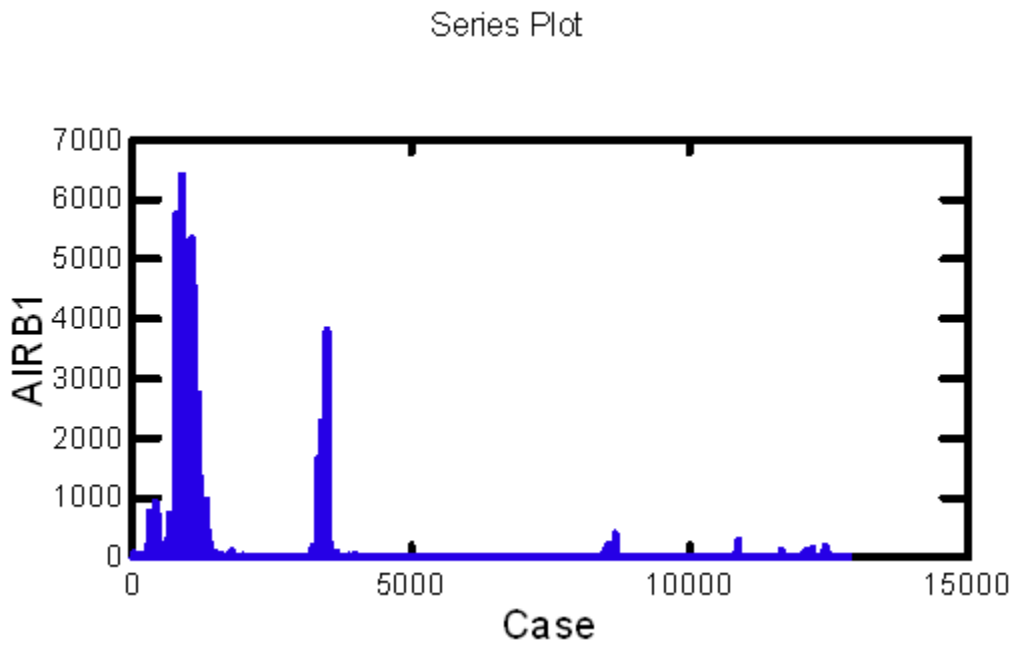
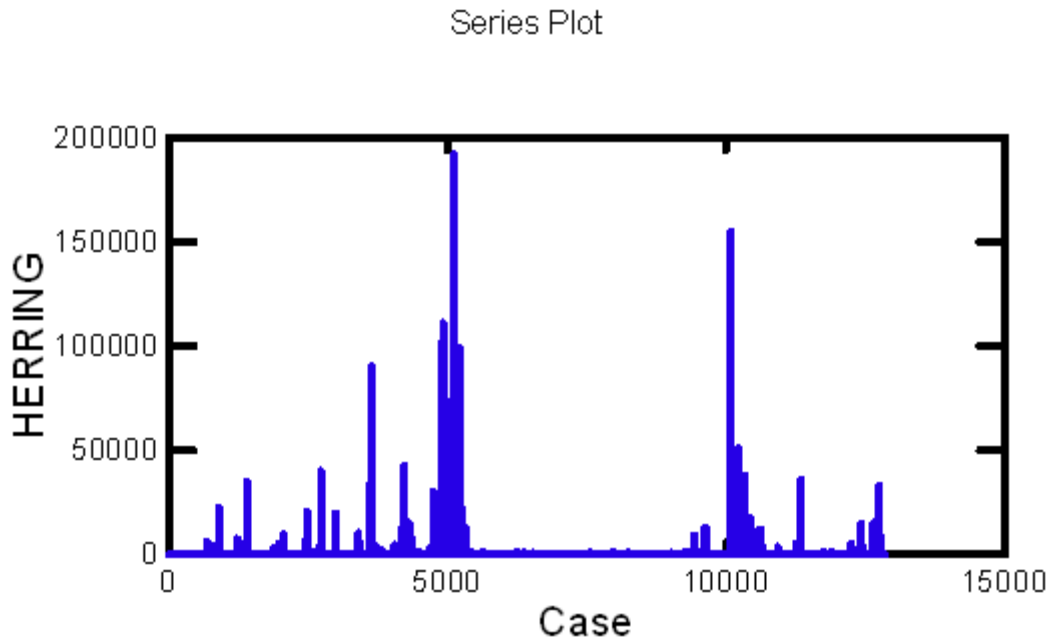


Figure 4. Time series plots of HERRING NASC (upper) and AIRB NASC, showing that it was in the start of the survey, with low Herring backscattering that the bubble attenuation was large, and therefore have insignificant effect on the survey results.

Egil Ona  
Kings Bay 23.02 2019

## REFERENCES

- Berg, T., Løvik, A. & Dalen, J. 1983. Increased precision of echo integration recordings under various weather conditions. *FAO Fish. Rep.* 300: 45-51.
- Dalen, J. & Løvik, A. 1981. The influence of wind induced bubbles on echo integration. *J. Acoust. Soc. Am.*, 69(13), 1653-1659.
- Forbes, S.T. & Nakken, O. 1972. Manual and methods for fisheries resource survey and appraisal. Part 2. The use of acoustic instruments for fish detection and abundance estimation. *FAO Man. Fish. Sci.* 15):138pp.
- Hall, M.V. 1989. A comprehensive model of wind-generated bubbles in the ocean and predictions of the effects on sound propagation at frequencies up to 40 kHz. *J. Acoust. Soc. Am.*, 89(13):1103-1117.
- Knudsen, H.P. 1990. The Bergen Echo Integrator: an introduction. *J. Cons. int. Explor. Mer.* 47:167-174.
- Knudsen, H.P. 2010. Bubble sweep down. Presentation at Workshop on bubble sweepdown, Kiel, Germany, March 16. 2010.
- Novarini J. C. and D. R. Bruno. 1982. Effects of sub-surface bubble layer on sound propagation. *J. Acoust. Soc. Am.* 72(2).
- Ona, E. 1987. Attenuation of sound energy from air bubbles in bad weather, and the correction of integrator readings. Internal report IMR, Bergen, Mar 14. 1987: 1-5. [ In Norwegian ]
- Ona, E. & Mamylov, V. 1988. Scientific report on cooperative work between Norwegian and Soviet specialists, May 19 - June 2, 1988, PINRO, Murmansk, USSR., 1-22.
- Ona, E. and J. Traynor. 1990. Hull mounted, protruding transducer for improving echo integration in bad weather. International Council for the explorations of the sea. C.M. 1990/B: 31.
- Ona, 1991. Vessel heave, and index for air bubble attenuation corrections. ICES. CM. 1991/B:37, 1-8.
- Shabangu, F.W., Ona, E., Yemane, D. (2014) Measurements of acoustic attenuation at 38 kHz by wind-induced air bubbles with suggested correction factors for hull-mounted transducers Fisheries research 151, 47-56
- Slotte, A. and H. Peña. 2005. Estimating the summer distribution and abundance of herring and blue whiting in the northern Norwegian Sea. Acoustic survey with "Hardhaus", Survey I: 13-27 June. Internal report Institute of Marine Research.



#### Annex 4. TS measurements

As in the 2016, 2017, and 2018 special investigations were made from MS Kings Bay in order to investigate the mean target strength, TS, of herring during the spawning migration. At two locations, detailed TS measurements was collected from the vessel transducers, by resetting the echo sounder to ping at 5 Hz to 100 meters without bottom detectors. (see echogram).

At one location, a Simrad WBAT, portable EK80 using a 38 khz and a 70 Khz split beam transducer were lowered into a layer of spawning herring at about 50 to 100 m depth, transmitting alternate series of 100 pings at each frequency at high PRF over two hours. The WBAT system was hanging from a surface buoy with positional devices and was left on drift by the vessel. Trawling and surveying the layer was conducted at 2-4 nautical miles distance from the buoy until the measurement were finalized. Results from these TS measurements will be analyzed on a later stage and is not included in the report. The idea behind these investigations is that a new depth dependent TS will be developed and used to re-estimate all years of this survey. This will be a more realistic TS and the depth term is also expected to remove potential bias related to variable depth distribution of the herring. The WBAT system was calibrated in Tromsø February 24, 2019.



Fig 1. WBAT system lowered into schools

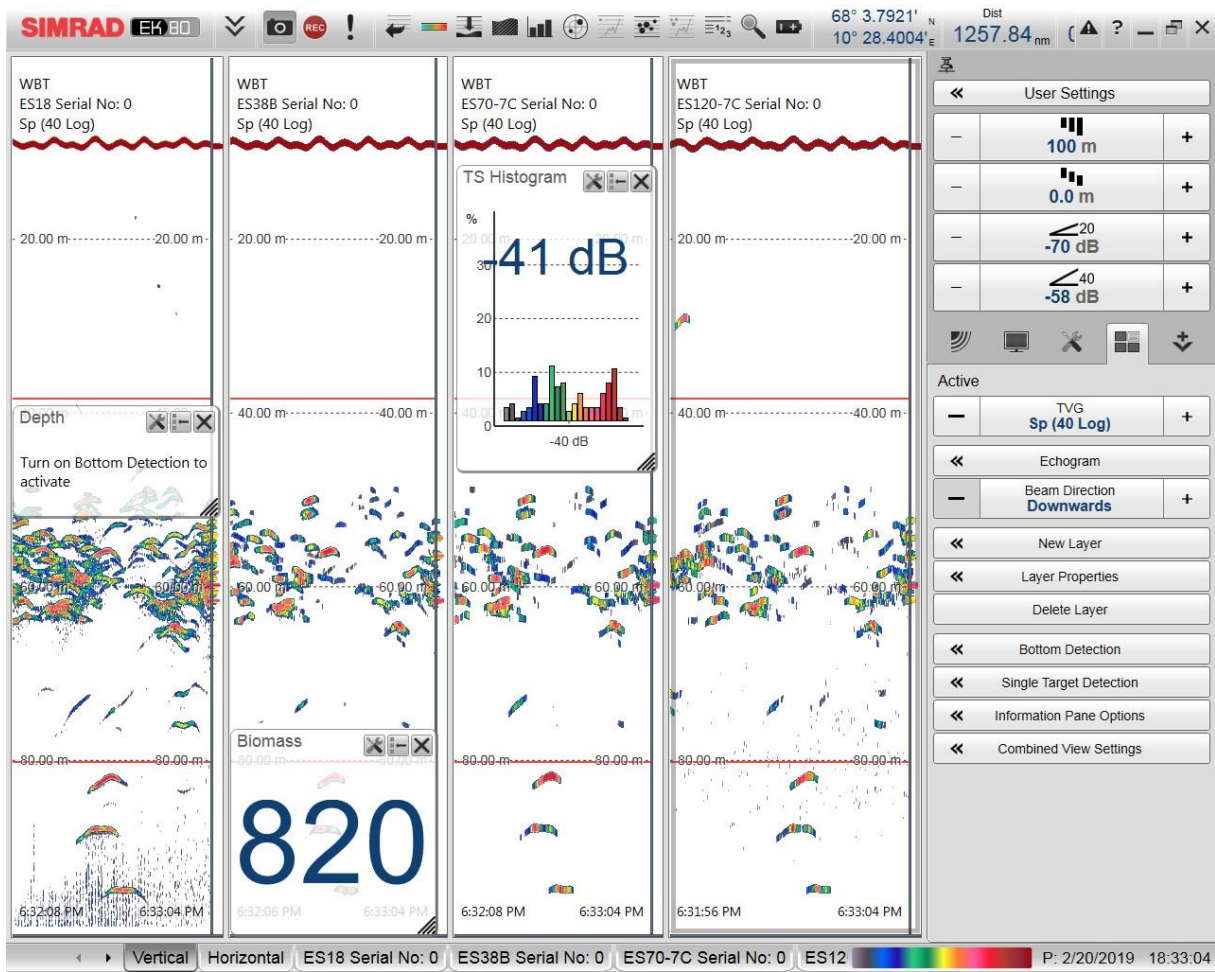


Fig. 2 TS measurements from vessel at 18, 38, 70 and 120 kHz

Annex 5. Examples of acoustic registrations with EK80 at Kings Bay

